Aalborg Universitet

AALBORG UNIVERSITY
DENMARK

Over-The-Air Testing Metrology of 5G Radios

Fan, Wei; Kyösti, Pekka; Jing, Ya; Wang, Zhiqin

Published in:
Metrology for 5G and Emerging Wireless Technologies

DOI (link to publication from Publisher):
10.1049/PBTE099E_ch10

Publication date:
2021

Document Version
Other version

Link to publication from Aalborg University

Citation for published version (APA):
Fan, W., Kyösti, P., Jing, Y., & Wang, Z. (2021). Over-The-Air Testing Metrology of 5G Radios. In T. H. Loh (Ed.), *Metrology for 5G and Emerging Wireless Technologies* (pp. 285-326). Institution of Engineering and Technology. https://doi.org/10.1049/PBTE099E_ch10

General rights
Copyright and moral rights for the publications made accessible in the public portal are retained by the authors and/or other copyright owners and it is a condition of accessing publications that users recognise and abide by the legal requirements associated with these rights.

- Users may download and print one copy of any publication from the public portal for the purpose of private study or research.
- You may not further distribute the material or use it for any profit-making activity or commercial gain
- You may freely distribute the URL identifying the publication in the public portal -

Take down policy
If you believe that this document breaches copyright please contact us at vbn@aub.aau.dk providing details, and we will remove access to the work immediately and investigate your claim.

Downloaded from vbn.aau.dk on: May 22, 2024

Chapter 1

Over-The-Air Testing Metrology of 5G Radios

Wei Fan[1] Pekka Kyosti[2] Ya Jing[3] and Zhiqin Wang [4]

1.1 Introduction

5G new radio (NR) (i.e. the global 5G standard) is introduced to significantly improve wireless system performance in terms of spectral efficiency, coverage, data-rate, latency, number of connected devices and energy efficiency. As 5G matures, now is the time for its large-scale deployments and commercialization. Several key radio technologies have been introduced to enable the 5G NR, e.g., high operating frequency (e.g, millimeter-wave (mm-wave) frequency), wider system bandwidth as compared with 4G, large-scale antenna configuration, and integrated radio frequency (RF) front-end design. Thorough testing of 5G NR radios is essential before their massive roll-out. Testing is required in the stage of device troubleshooting, regression, validation and performance evaluation. However, these NR technology advances have posed significant challenges on testing methods. Test complexity has significantly increased due to higher operating frequencies, wider system bandwidth, increased minimum number of test cases, increased overall test time, electrically larger antenna under test (AUT) and necessity of over-the-air (OTA) testing.

Traditional cable conducted testing is getting problematic due to complexity introduced in advances RF and antenna technologies. Components of radio devices, including the modem, RF circuits and antennas were individually designed and separately tested in the traditional conducted test setup. However, integrated RF front-end design is expected in the 5G NR due to cost, size and design consideration. If RF coaxial cables and connectors, which are not part of the final wireless product, are employed during the testing, they introduce losses and mis-matches and may also intrusively affect the radiation pattern profile of the wireless product under test. Antenna ports, if accessible, become massively bulky due to large-scale antenna array configuration, which makes traditional cable conducted testing complicated, expensive and error-prone. Furthermore, many benefits of 5G NR systems are introduced by the spatial discrimination capability of their employed antenna arrays (e.g. beam-

[1]Aalborg University, Denmark
[2]Oulu university and Keysight technologies, Finland
[3]Keysight technologies, China
[4]China Academy of Information and Communications Technology, China

forming towards desired signal directions and null steering towards undesired directions), which cannot be measured accurately at each antenna element port. Therefore radiated OTA testing, where built-in antennas are used directly as the interface to receive/transmit test signals, will be the main-stream method for 5G radios, especially for radios operating at mm-wave bands and above.

In this book chapter, the focus is given on OTA testing methodologies of 5G radios. The first part focuses on the wireless system performance testing, where the objective is to evaluate 5G radio performance, e.g. throughput, under realistic spatial channel conditions. Two standard OTA testing methods, namely the multi-probe anechoic chamber (MPAC) and radiated two-stage (RTS) method are detailed. The second part focuses on the RF testing, where the goal is to test 5G RF parameters under ideal plane wave conditions. The focus is given on a novel mid-field testing method. Other mature RF testing methods, e.g. direct far field (DFF), compact antenna testing range (CATR), plane wave generator (PWG) and near-field to far-field transformation (NF-FF) method, can be found in many references in the literature and therefore are not detailed in this book chapter. The third part introduces the current status of OTA testing of 5G radios in standardization, where both wireless system performance testing and RF testing are discussed.

1.2 Performance testing

1.2.1 Introduction

When wireless communication devices, e.g., mobile phones, are under development or being manufactured, it is typically mandatory to test if their radio performance meets the requirement or specification under realistic propagation conditions. A natural and intuitive way to test it is to measure the performance of the device-under-test (DUT) in the live network of different scenarios, e.g., urban or suburban scenarios. This is the so-called field trials. Field trials do tell the real-world performance of DUTs, but they often suffer from the uncertainty introduced from the environment. The test results may not be repetitive due to, e.g., various weather conditions and propagation phenomenon. The variation of the test results makes it difficult to judge if a DUT is qualified in regard to the designed specification. Moreover, it is also unfair to compare the test results of different DUTs in field trials due to any potential changes in the propagation channel.

To make the test results both representative of real-world performance and comparable between different DUTs, an alternative, i.e. virtual drive testing, is often adopted in the industry. Virtual mobility testing can be thought of as doing the aforementioned field trials in a more controllable, repeatable, and reproducible manner by "emulating" the propagation channel to laboratories. The propagation channel can be emulated according to the standard channel models that are widely adopted for testing. With virtual mobility testing, different DUTs can be tested under exactly the same channel, and hence the test results are more repeatable, and the comparison of the test results is fairer.

Conventionally, virtual mobility testing has been done in a conducted manner, where radio signals are sent over coaxial cables. This is called the conducted testing. A basic setup of the conducted testing consists of three components, including a signal generator which generates the test signal, a channel emulator which generates the wanted propagation channel and performs convolution between the test signal and the channel, and lastly the DUT which receives and demodulates the faded test signal. All three components are wired up with coaxial cables.

Though the setup is very simple and straightforward, there are a few disadvantages to it. Firstly, the DUT is fed with the test signals via cables, which is done at the antenna ports in the DUT. This means the original enclosure of the DUT has to be opened, and the antennas inside the DUT need to be unmounted to give the port-to-cable connections. The manual handling could be tedious and time-consuming, especially with mass volume testing. Moreover, when the antenna module is directly integrated to the logic board, which means there is no antenna ports available for cable connection, i.e. the conducted testing become impractical. Secondly, the effect of the antenna radiation pattern is accounted for in the channel emulator when generating the wanted channel coefficients. Nevertheless, the radiation pattern would need to be measured beforehand. If the radiation pattern is measured with the antenna module alone, the resulting radiation pattern may not reflect the influence of, e.g., the chassis and other components of the DUT, which may cause discrepancy on the antenna radiation pattern in reality, and hence compromise the effectiveness of the test results. Some DUTs may support the so-call antenna test functions, which allows us to measure the antenna radiation pattern on-board. In this case, the discrepancy of the measured antenna radiation pattern to the reality can be minimized.

Due to these reasons, the testing community has been moving to an OTA manner. However, since the desired radio signals are not guided to the DUT over cables as in the conducted testing, methods to achieve similar effects are needed for the OTA testing. How to emulate a channel OTA according to standard channel models with high fidelity in the test environment becomes the research focus of multiple-input-multiple-output (MIMO) OTA testing. Many OTA techniques have been proposed in the literature and selected in the standard covering different real-world operating scenarios. Though OTA testing is more complicated than that for the conducted testing, they offer some appealing features such as being non-intrusive to DUTs and providing realistic radio interaction with the DUT as if in real life. Below, the discussion is focused on two standard OTA testing methods for system performance testing, i.e. the MPAC solution and the RTS solution.

1.2.2 MPAC solution

1.2.2.1 Background

Current MPAC OTA test methods have their roots in the measurement specification for single antenna system by the International Association for the Wireless Telecommunication Industry (CTIA) [1]. Two test metrics, namely Total radiated power (TRP) and Total isotropic sensitivity (TIS), were defined for the transmitter and receiver performance evaluation of a user equipment (UE) in the active mode, re-

spectively. The relation to MPAC methods is two-fold. Firstly, both measurements can be done using multiple probes, though only one of them is active at a time for single-input single-output (SISO) OTA testing, while all probes are activated simultaneously in the MPAC setup for emulating the spatial channels. Secondly, the DUT is operating in its normal (active) mode and the intermediate metric in TIS is the link throughput, which is not a direct RF parameter. TRP measures how much power the DUT, together with its RF parts and antennas, can radiate overall. TIS measures the receiver sensitivity of the DUT, i.e., the minimum power level when a certain throughput can still be achieved. Especially, TIS evaluates the DUT as a whole, with its baseband, RF, and antenna capability. These tests can be performed either in an anechoic chamber (AC) with single or multiple probes, or in a reverberation chamber (RC). In AC there were similar research questions as in current MPAC systems, e.g., what is the sufficient range length, i.e., the distance between DUT and probe(s), and how many DUT orientations are to be measured to capture the isotropic condition.

With the introduction of multi-antenna UEs and use of MIMO techniques, it became evident that good or bad antenna designs cannot be assessed with the existing SISO OTA performance evaluation. For example, a UE with two high efficiency antennas, but with similar polarizations and short inter-element distance, is not optimal for diversity or spatial multiplexing schemes, due to the possible high antenna correlation at the two antennas. By MIMO techniques we do not mean here only the spatial multiplexing, but any diversity or beamforming schemes. The incapability of previous OTA methods to test such simple MIMO operation as diversity switching was recognized and consequently the need for new test concept has been identified [2]. Moreover, it was remarked that antennas and other functional blocks of MIMO transceivers cannot be tested separately, since MIMO communications is highly dependent on the radio channel conditions. A static line-of-sight channel with averaging over many orientations (as done for the SISO OTA testing) does not give insights to the overall performance of multi-antenna terminals. Temporally varying radio channel with polarimetric and angular dispersion is needed for the evaluation of multiple antennas and MIMO processing. The concept of MPAC with anechoic chambers, channel emulators, and multiple dual polarized probes in different angles with respect to the DUT, was sketched in [3]. A similar concept was published a bit earlier in [4].

The aforementioned is one perspective to the development of MIMO OTA testing. This perspective considers the evolution of antenna tests and measurement practices. Another perspective is related to the development of traditional conductive testing of baseband functionalities of MIMO capable devices. Radio channel models had been defined for MIMO evaluations in fading channel conditions. The question was how to extend these tests to incorporate antennas and corresponding RF designs. The question became unavoidable at latest in the advent of mm-wave frequency transceivers and disappearing of physical antenna connectors. MIMO capable devices had been tested with channel models and fading emulators in a conductive mode, i.e., not OTA, connecting the test equipment to DUT with RF cables. The traditional conductive MIMO emulation is briefly introduced in the following

sub-section. After that, we move to discussing how the same emulation functionality is pursued OTA.

1.2.2.2 System function of conductive MIMO emulation

The system model in [5] is

$$\mathbf{Y}(t,f) = \mathbf{H}'(t,f)\mathbf{X}(t,f) + \mathbf{N}(t,f), \tag{1.1}$$

where $\mathbf{Y}(t,f) \in \mathbb{C}^{(N1)}$ is the received signal vector, $\mathbf{H}'(t,f) \in \mathbb{C}^{(NM)}$ is the MIMO channel transfer function, $\mathbf{X}(t,f) \in \mathbb{C}^{(M1)}$ is the transmitted signal vector, $\mathbf{N}(t,f) \in \mathbb{C}^{(N1)}$ is the noise vector at receiver inputs, and N, M denote the number of receiver (Rx) and transmitter (Tx) antenna ports, respectively. MIMO channel model with L paths can be defined as

$$\mathbf{H}'(t,f) = \sum_{l=1}^{L} G_{rx}\left(t,\Omega_l^{rx}(t)\right) \begin{bmatrix} \alpha_l^{\theta\theta}(t,f) & \alpha_l^{\theta\phi}(t,f) \\ \alpha_l^{\phi\theta}(t,f) & \alpha_l^{\phi\phi}(t,f) \end{bmatrix} G_{tx}\left(t,\Omega_l^{tx}(t)\right)^T, \tag{1.2}$$

where $\mathbf{G}_{rx} \in \mathbb{C}^{(N2)}$ and $\mathbf{G}_{tx} \in \mathbb{C}^{(M2)}$ are the antenna pattern matrices of θ and ϕ polarizations for Rx and Tx antenna arrays, respectively. Furthermore, α_l^{ab} are time t and frequency f selective fading complex channel gains of path l for received polarization a and transmitted polarization b, Ω_l^{rx} and Ω_l^{tx} are the arrival and departure solid angle of path l, respectively. The formulation of Equation (1.2) enables polarimetric and spatially selective fading MIMO channels. Each row of an antenna pattern matrix $\mathbf{G}$ is composed of one or several physical antenna elements that are fed from baseband unit only with a single RF chain. Antenna patterns are time variant, e.g., in the case of analogue beamforming sub-arrays with time variant weights or adaptive switching of antennas.

Equation (1.1) is defined in frequency domain for mathematical convenience. Normally standard channel models are determined and fading emulation performed in delay (-time) domain, which is achievable by Fourier transformation over the frequency dimension. Transmitted signal vector, originated from a test equipment, is directed to fading channel emulator (CE) through M RF ports with coaxial cables. CE performs convolution with vector $\mathbf{X}$ and channel matrix $\mathbf{H}'$ and outputs signal vector $\mathbf{Y}$ through N coaxial cables for the RF input ports of the DUT. With properly calibrated test system it is possible to emulate $\mathbf{H}'$ shown in Equation (1.2) on high precision, i.e., to test the DUT in channel conditions defined by the target channel model. Even though DUT antennas are bypassed by RF cables, their approximate model can be included in the emulation by defining $\mathbf{G}_{rx}$. In practise it is difficult to include all coupling and other RF effects perfectly in the model.

1.2.2.3 Principle of MPAC

The MPAC test setup is composed of a digital fading emulator, an anechoic chamber and a set of OTA probe antennas. It is initially described in [6] and thoroughly in [7]. The intention in MPAC OTA test setup is to generate time variant electromagnetic fields with specified angular, polarimetric and delay dispersion characteristics around the DUT. The characteristics follow target channel models that are, typically, defined to reflect realistic propagation conditions. Figure 1.1 illustrates el-

ements of the set-up. The DUT is in the centre of the anechoic chamber, in an area called test zone, and the probes are arranged, e.g., uniformly around the DUT in a two- or three-dimensional constellation. Each probe is connected to an output port of the CE, possibly thorough a power amplier. Amplification may be required between CE outputs and probes to compensate for the path loss between probes and the DUT. A communication tester generates the test signal that is fed to the CE. The CE performs the convolution of the channel model impulse responses and Tx signals. Thus, it constructs the multipath environment including path delays, Doppler spread and fast fading. The channel model, containing polarization characteristics and directions of departures and arrivals, is mapped to the CE such that the model allocation corresponds to the physical probe installation in the chamber. The DUT is assumed to be in the far field region of each probe, and vice versa. In the actual OTA test, an appropriate performance metric, e.g. throughput, is collected as a gure of merit. Target channel models define the temporal/Doppler, frequency/delay, space/angle, and polarimetric parameters of fading MIMO radio channel conditions. Standard channel models do not define, however, the instantaneous impulse or frequency responses of the channel.

The reconstruction of target field for the DUT is based on the following fact of the antenna measurement and EM theories. According to [8] a closed boundary, e.g., a spherical or cylindrical surface in the three/dimensional (3D) case or a circle in the two-dimensional (2D) case, determines the field within the boundary, when no sources are present inside the boundary. The intended target field results inside the test zone, if such a field is generated, where the components of both the electric and magnetic fields tangential to the surface of the test zone are equal to those of the target field [9].

Generally, both downlink and uplink transmissions and their fading emulation are required in active mode testing. In the simplest case no fading or multipath effects are emulated in the uplink. In this case an uplink communication antenna, connected

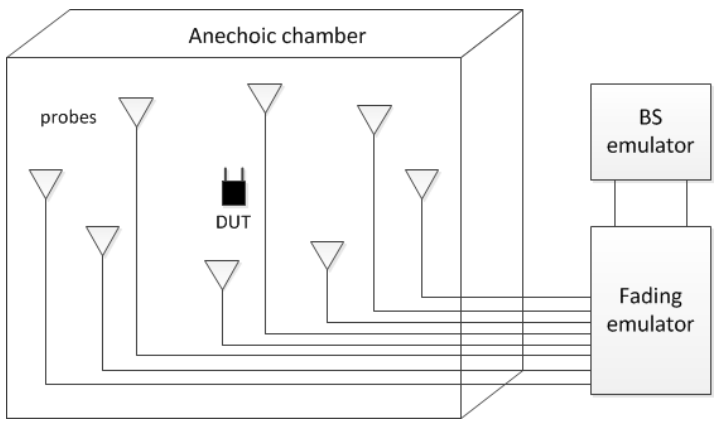

Figure 1.1: MPAC MIMO OTA test set-up containing fading emulator, anechoic chamber, and multiple probes (Fig. 1 in [7]).

to the communication tester with a coaxial cable, is located inside the AC such that it does not distract any probe - test zone clearance. In time division duplex (TDD) systems the uplink radio channel should be reciprocal with the downlink and thus both up- and downlink fading must be emulated. This can be achieved by receiving the uplink signals by probes and performing fading also for them within the CE.

Probes must be dual polarized when the polarization dimension of radio channel is considered. Both orthogonally polarized elements of a single probe, must be connected to different CE outputs. This will enable independent fading on different polarizations, which is required by most standard channel models. It is possible to generate any polarization states like, e.g., circular, linear, or elliptical with orthogonally polarized, co-located, and phase calibrated probe elements.

1.2.2.4 System function of MPAC OTA emulation

Assume a MPAC setup with K probes located around the test zone with a certain polarization, distance, and directions from the centre of the test zone. Assume the bore sight of probe antennas is pointing towards the test zone. We can construct similar MIMO system function as Equation (1.1) from the Tx antenna ports to the Rx, i.e. the DUT [5], antenna ports. Now the MIMO channel is not determined only by a calibrated CE running the target channel model containing specific Tx and Rx antenna models. Instead, the transfer function is composed jointly by the CE with a channel model in it, cables, probes, propagation environment within the AC, and DUT antennas. Some of these components are typically partly or completely unknown and there is no intention (or means) to fully determine the unknowns by any calibration measurement.

In MPAC setup the matrix $\mathbf{H}'$ in Equation (1.1) is substituted by

$$\mathbf{H}(t,f) = \mathbf{F}(t,f)\mathbf{W}(t,f), \tag{1.3}$$

where the first term $\mathbf{F} \in \mathbb{C}^{(NK)}$ contains DUT antennas, the AC, and probes, i.e. the physical environment within the AC from K probes to N DUT antennas. Entries of matrix $\mathbf{F}$ are

$$\Psi(t,f) = \mathbf{G}_{rx,n}(t,-\vec{\beta}_{n,k})\mathbf{G}_{o,k}(\vec{\beta}_{n,k})^T \frac{\lambda}{4\pi d_{n,k}} e^{j\beta d_{n,k}}, \tag{1.4}$$

where $\mathbf{G}_{rx,n}$ and $\mathbf{G}_{o,k} \in \mathbb{C}^{(12)}$ are the polarimetric antenna pattern vectors of DUT antenna n and probe k, respectively. The direction and frequency are specified by the wave vector $\vec{\beta}_{n,k}$ from probe k to DUT antenna n. The corresponding distance is denoted by $d_{(n,k)}$. Finally, λ and β are the wavelength and the wave number, respectively. As mentioned previously, DUT antennas may have time dependent radiation patterns due to possible analogue beamforming or antenna switching.

The second term $\mathbf{W} \in \mathbb{C}^{(KM)}$ of Equation (1.3) is a specific OTA channel model executed in the CE. It contains the time and frequency selective fading propagation

[5] In this section we label DUT as the receiver and the other link end the transmitter for notational clarity. In practice, however, both link ends transmit and receive signals in the active mode.

coefficient $\alpha_{(l,k)}^{ab}$, Tx antenna radiation patterns $\mathbf{G}_{tx}$, and specific OTA probe weights $\gamma_{(l,k)}^{a}$. The kth row, $k = 1, \cdots, K$ of matrix $\mathbf{W}(t,f)$ is

$$\mathbf{W}(t,f) = \sum_{l=1}^{L} \begin{bmatrix} \gamma_{l,k}^{\theta} & \gamma_{l,k}^{\phi} \end{bmatrix} \begin{bmatrix} \alpha_l^{\theta\theta}(t,f) & \alpha_l^{\theta\phi}(t,f) \\ \alpha_l^{\phi\theta}(t,f) & \alpha_l^{\phi\phi}(t,f) \end{bmatrix} G_{tx}\left(t, \Omega_l^{tx}(t)\right)^T . \tag{1.5}$$

Now the challenge is to determine weights $\gamma_{l,k}^{a}$ and fading coefficients $\alpha_{(l,k)}^{ab}$ such that DUT within the test zone experiences characteristics of the target channel model. These targeted characteristics are, e.g., the power delay profile (PDP), Doppler spectrum, Ricean K-factor, amplitude distribution, cross polarization power ratio, and power angular distribution as observed by the DUT.

1.2.2.5 Field synthesis methods

Two alternative methods can be used for reproducing fading radio channel conditions within a test zone. They are called the plane wave synthesis (PWS) and the pre-faded synthesis (PFS). These methods set slightly different requirements for the setup and provide different capabilities, while in many cases they lead to statistically similar channel emulation.

Plane wave synthesis

The static target field inside a sufficient small test zone can be controlled by tuning the phases and amplitudes of fields radiated by the probes [7]. The MPAC setup must be phase and amplitude calibrated and the transfer functions to the centre of the test zone must be known. Then different field shapes, i.e., polarizations, amplitudes, and phase-fronts can be controlled by setting complex excitation coefficients $\gamma_{l,k}^{\theta}$ and $\gamma_{l,k}^{\phi}$ in the fading emulator for signals routed to the probes. Any field structure can be decomposed to the contribution of plane waves with different directions, phases, and amplitudes. Moreover, standard channel models typically define geometric channels with rays, that can be interpreted as plane waves. Hence, the basic field component in PWS is the plane wave. The principle of plane wave generation in the two-dimensional space is depicted in Figure 1.2.

A Doppler frequency can be introduced to plane waves by introducing a time-variant phase term. The polarization state is set by using dual polarized probes and controlling relative phases and amplitudes of orthogonal polarization components. Any number of plane waves with different directions and temporal characteristics can be generated without extra complexity. This enables the reconstruction of any instantaneous radio channel conditions and arbitrary power angular spectra (PAS) [11]. Path delays and time variability are generated by the fading emulator.

Pre-faded synthesis

The approach of the PFS is different, though it uses same HW resources and results in statistically equivalent emulation in the case of many standard channel models. The PFS does not aim to control instantaneous EM fields exactly and does not require phase calibration [7]. Instead, it controls the power angular distribution and the polarization power ratios as observable by the DUT. Time/Doppler and de-

lay/frequency domain effects are generated in the fading emulator, similarly to the PWS method. Weight coefficients $\gamma_{l,k}^{\theta}$ and $\gamma_{l,k}^{\phi}$ of Equation (1.5) are real-valued amplitudes in PFS [12]. The PFS method suits well for channel models with cluster definition of propagation parameters, such as the 3rd generation partnership project (3GPP) models for 4G and 5G evaluations.

1.2.3 Research/Design questions

The design of an MPAC test system must balance between the system precision and system complexity (and cost). Many research questions rise from the specification and designing of a MPAC system. What is the minimum number of probes needed for a certain DUT category? What is the minimum range length and consequently the minimum AC size? Where, i.e., to which directions, to place the limited number of probes? How to determine weights $\gamma_{(l,k)}$ for a specific channel model? These questions are briefly discussed in the following sub-sections.

1.2.3.1 MPAC configuration

The measurement range is an important aspect for system design, as it determines the chamber size (which is a major cost determining factor of the setup). The requirement on the measurement range for mm-wave antenna array is extensively discussed in [13]. It was concluded that the far field distance based on the maximum device dimension is not supported by the system link budget. Results have indicated that shorter distances than the far field distance can still yield reasonable measurement accuracy for antenna array and MIMO related metrics for testing purposes. The range length is an active discussion item within 3GPP.

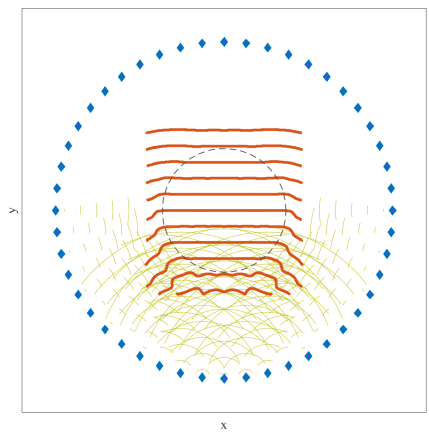

Figure 1.2: Construction of a 2D plane wave with PWS (Fig. 2 in [10]).

The OTA antenna configuration (i.e., number and locations of OTA antennas) are mainly determined by the required radio channel emulation accuracy in the test zone. The radio channel emulation algorithm in MPAC test systems (i.e. mapping radio channel models to multiple OTA antennas, using e.g. the plane wave synthesis (PWS) technique or the pre-faded signal synthesis technique.) has been extensively investigated for sub-6 GHz MIMO OTA testing. The cost of the MPAC setup is also determined by the channel emulator resource and the number of probes required for reproducing the target spatial channel models.

MPAC setups using either of the synthesis methods aim at an angular sampling of the test zone by probes so that a perfect reconstruction of the target PAS is achievable. Different approximations for estimating the number of probes or the minimum angular sampling to reach the goal have been reported. The cut-off property of a spherical wave series gives the following rule of thumb [9] for the required probe number K for a uniform 2D setup

$$K = 2\lceil 2\pi r \rceil + 1, \tag{1.6}$$

where $\lceil \cdot \rceil$ is the integer ceiling operator and r is radius of the cylindrical test zone in wavelengths. The maximum increment of the angular sampling by probes is consequently

$$\theta_\Delta = 360^\circ / K. \tag{1.7}$$

It has been demonstrated that a large number of probes is required to create a large test zone. Setting up a 3D MPAC configuration for 5G radio devices is costly, so finding ways to limit the number of probes while still approximating the target channels sufficiently accurately could make the test system both cheaper and simpler to implement. Inspired by the fact that radio channel models are generally directional in real world scenarios, probe selection framework is generally adopted for MPAC setup for 5G radios [14–16]. A uniform configuration of the OTA probes is not ideal and a probe selection mechanism can save cost, via reducing the required number of fading channels. This way, the associated RF chains can be effectively reduced to save cost. This concept is also adopted for the MPAC setup for 5G frequency range 2 (FR2) testing in the standardization.

For any OTA test system, we need to define testing metrics to evaluate how well the desired propagation channels are reconstructed. We can directly compare, e.g. the continuous target PAS and the discrete emulated PAS implementation using a limited number of probes in the MPAC setup. For sub-6 GHz systems, the PAS deviation is indirectly evaluated via the spatial correlation. That is, the spatial correlation calculated from the target spatial channel models is used as reference to judge the accuracy of emulated spatial correlation in the MPAC setup. For 5G beam-steerable devices, beam probability, which is adopted to characterize the beam selection performance of the mm-wave antenna system under spatial fading channels, can be utilized [14, 15]. Another metric for 5G radios is the beamforming power spectra similarity, which is the similarity of the target PAS and the discrete PAS reproduced in the OTA test system as seen by the DUT [14, 15].

1.2.3.2 Channel emulation method

The determination of complex excitation coefficients in the PWS method are discussed, e.g., in [7] and [11]. The principle is to define the target field in a set of sample points within or around the test zone, to specify the transfer function from K to all sample points, and to solve excitation coefficient from the determined set of linear equations. This is typically done for a set of plane waves, apparently arriving to the DUT from different directions.

In the case of the PFS, the probe weights are determined to reconstruct the power angular spectrum of the target channel model. In 4G systems this was usually done by using the spatial correlation, or more specifically the error between the target and the reconstructed spatial correlation function within the test zone, as the metric to be minimised [7]. In 4G devices the MIMO techniques were mainly spatial multiplexing and diversity. This made the spatial correlation between, possibly, widely spaced DUT antenna locations a meaningful metric. Recall the Fourier transformation link between the power angular spectrum and the spatial correlation function. In 5G mm-wave systems the primary use of multiple antennas is beamforming. Hence, a potential metric for weight determination could be a deviation between the target and the reconstructed power angular spectrum, as observable by an ideal antenna array. This metric is called the PAS similarity percentage and it is defined in [5].

The comparison between the PWS and PFS is performed for implementing geometry based stochastic channel models (GSCMs) [17]. It shows the cluster-wise channel emulated by the PFS method is Kronecker structured, which is different from the general definition of GSCMs. In contrast, the channel emulated with the PWS method is consistent with GSCMs. Moreover, the emulation accuracy for the two methods are compared under different target channel settings, i.e. different cluster angular spreads. The simulation results demonstrate the advantage of the PWS method over the PFS method, especially when cluster angular spreads are small.

1.2.3.3 Channel Validation

The objective of the channel validation measurement is to ensure that target channel models are correctly implemented inside the test area in the MPAC setup. Several aspects of the emulated channel models are analyzed in the channel validation measurements, including the fading distribution, PDP, power Doppler spectrum/temporal autocorrelation function, spatial correlation, and cross-polarization ratio. The spatial correlation, which is a statistical measure of the similarity between received signals at different spatial locations, has been used to represent the channel spatial characteristics at the receiver side and is selected as the figure of merit (FoM) for OTA testing in conventional MPAC setups. The spatial correlation might be less relevant to determining OTA system performance for beam-steerable devices; the PAS of the emulated channels are more interesting. Therefore PSP is used in the FR2 to measure the similarity of the PAS produced by the MPAC system and the reference PAS in the target channel model. Research works have also been reported to validate the joint-angle delay power profile of the emulated channels in the MPAC setup [18].

Validation of spatial fading channel emulation in 5G frequency range 1 (FR1) has been extensively discussed in the literature and a preliminary work has been

reported on validation in the FR2 chamber [19]. There are some practical difference of validation at the FR1 and FR2 chamber. The probe antennas and measurement antennas are more directive at the FR2. Virtual array, which is used to estimate the emulated channel spatial profile in the chamber, will be more difficult to form with the mechanical positioner, as the wavelength at the FR2 is much smaller. The channel emulation at FR2 is also more complicated, which involves frequency up-and-down conversion for the sub-6 GHz channel emulator. Spatial correlation and power angle spectrum were investigated for the simple MPAC setup in the FR2 chamber in 19. An excellent agreement between the measured results and the target is achieved in terms of spatial correlation and power angle spectrum, which validates the MPAC method in the mm-wave bands in the FR2 band.

1.3 Two-stage MIMO OTA test method

1.3.1 Principle of the Radiated two-stage method

The basic concept of the Two-Stage MIMO OTA test method is to divide the OTA test into two stages: the first stage is to acquire the antenna pattern of DUT, the second stage is to perform the throughput measurements using a downlink signal generated by convolving the device antenna pattern with the desired spatial channel model through a conducted or radiated connection. This innovative idea was first proposed to 3GPP RAN4 meeting in 2009 in [20] with the conducted second stage throughput test, and more analysis and test results are summaries in [21]. The radiated version of the RTS was proposed to 3GPP in [22] to overcome the shortcomings of cable-conduct throughput test and finally accepted by 3GPP and CTIA as one of the standardized MIMO OTA conformance test methods [23–25]. Several Papers have already been published to introduce Two-stage MIMO OTA method from different aspects [26–29].

In the first stage, the DUTs antenna pattern can be acquired, depending on the test context, by simulation, design or measurement of the actual DUT antenna pattern. To overcome the shortcomings of the presence of the connecting cables, for example, the integrity of the device is altered and changes in the impedance seen by the antennas, Two-Stage method employs a non-intrusive antenna measurement method which does not require the connection of cables. This non-intrusive antenna measurement approach uses the ability of the receiver in the DUT to measure the amplitude and relative phase of known signals received by DUT antennas. The amplitude and phase information can be collected in two ways: Layer 3 messages or user datagram protocol (UDP) packets. For Layer 3 message method when Base Station emulator sends the antenna measurement request in downlink Layer 3 message, the DUT reports the received signals power and phase information in uplink L3 message following the format described in [30]. For the UDP method one antenna measurement app should be pre-installed on DUT and launched after the call connection is setup. When the app receives the antenna measurement request from test PC, the received signals power and phase information is assembled into UDP packets and sent out to test PC with specified IP address and port number. By ro-

tating the DUT relative to the known incident signal it is possible to construct the 3D antenna patterns with amplitude and phase responses. To fully characterize the antennas, measurements are made at two orthogonal probe antenna orientations, typically vertical and horizontal. This can be done by switching between two separate antennas or by rotating a single antenna.

In the second stage the desired antenna pattern is loaded into a channel emulator and convolved with the spatial channel model being used to evaluate the DUT performance. How the antenna pattern is embedded into the channel model will be introduced in the followed section. This process generates the signals at the DUT receiver that would have been received had the DUT been placed in the same 2D or 3D spatial field used for the convolution. During the second stage it is not necessary to alter the device orientation relative to the probe antennas since the rotation of the DUT relative to the chosen channel model is performed electrically within the channel emulator. In this stage there are two options for connecting the signal generated by the channel emulator to the device. The simplest is to use cables connected to the devices temporary antenna connectors should they be available shown as Figure 1.3. This is usually not a problem for traditional RF test but is becoming increasingly more difficult on mobile devices where space is at a premium. When goes to FR2 mm-wave frequency even there are no available RF connectors. The conducted second stage does not require the use of an anechoic chamber for the throughput measurements although some form of RF shielding is desirable to prevent any ambient interference from affecting the results. A consequence however of using the cabled connection is that any radiated interference generated by the device which would otherwise have desensitized the receiver through its own antenna is no longer measured. When the device is operating at low transmit powers this is not an issue but at high power there may be differences in performance compared to radiated throughput measurements.

The alternative to a conducted second stage connection is to use a radiated ”cable replacement” connection shown as Figure 1.4, which is known as RTS method. This approach does require the use of an anechoic chamber for throughput measurements but has the benefit that any radiated interference generated by the device is fully considered in the measurements. The purpose of the radiated connection is to enable the signals generated by the channel emulator, which are already conditioned to include the effect of the device antennas, to be directly connected to the device

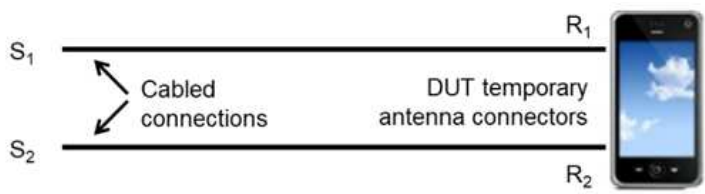

Figure 1.3: Cable-conducted second stage throughput test.

receiver. However, this can only be done by calibrating out the impact of the signal propagation in the anechoic chamber and the impact of the device antenna.

Many strategies have been reported in the literature to obtain the radiated channel matrix between the probe antenna ports and the DUT antenna ports, depending on the available output information from the DUT. As discussed in [31], the channel matrix can be directly calculated based on the knowledge of complex antenna patterns of the DUT. This method, however, typically requires a large anechoic chamber for far field antenna pattern measurement and support from a special chip-set to report DUT complex antenna patterns in a non-intrusive manner. This idea is detailed in the original RTS method. The channel matrix can also be directly estimated via channel estimation algorithms, e.g. utilizing pilot sequence. This idea, however, might only be supported by base station (BS) type DUT where transmitted signals can be designed and therefore known. In [32], based on the received Reference Signal Received Power (RSRP) value per DUT antenna port, a calibration method is proposed to determine the channel matrix. The method is highly attractive since the testing can be performed in a small RF shielded enclosure. The method was then extended for high-order MIMO DUT in [33], with a closed-form calibration method. The unique features of mm-wave antennas also open up new possibilities to achieve wireless cable connection. A straightforward way to achieve wireless cable connection is to design the radiated channel matrix in the multi-probe setup, saving the need to compensate it in the CE. For example, if the DUT can form widely-separated directive beam patterns, each towards a directive and direction aligned probe antenna, we can achieve cable-like connection OTA via antenna pattern discrimination. Alternatively, polarization discrimination is another way to achieve virtual cable connection for 2×2 MIMO systems. The wireless cable can be directly achieved via adopting orthogonality between two cross-polarized components, where two wireless cable connections can be achieved. In [19], two proposed schemes, i.e. polarization discrimination and antenna pattern discrimination, are two examples to approximate wireless cable connection. This strategy is not generic for any DUT, and in any multi-probe setup. For small mm-wave UEs, it might be not practical to design many widely separated beams due to design limitations. As for polarization discrimination case, it is only limited to 2×2 MIMO systems and MIMO handsets with two orthogonal linear polarized antenna designs. The more general calibration method, which can determine the radiated channel matrix $\mathbf{A}$ without relying on DUT antenna radiation properties and multi-probe setup, is therefore more generic to achieve wireless cable connection. Below we focus on the methods introduced in the original RTS method to achieve the wireless cable concept.

The advantage of this two-stage approach is that radio conditions representing arbitrarily complex 2D or 3D spatial channels can be completely emulated in channel emulator using a simple anechoic chamber with high accuracy. The required probe antenna number depends on the measured MIMO order. For example, if 2×2 MIMO is tested only two probe antennas are required. Another advantage is because of acquiring antenna pattern in first stage, more diagonal information can be got for performance debug. Except for antenna-only metrics such as gain, branch power imbalance, envelope correlation coefficient (ECC) etc, when the device antenna patter

is convolved with the spatial channel model including the Tx antenna assumptions that it is possible to see the actual signal that will be presented to the receiver for demodulation. Since the Two-stage method has access to all the elements in the Tx antenna, channel emulation and Rx antenna it is possible to compute a wide variety of signal characteristics that can help predict and explain the variation in DUT performance.

1.3.2 Applying measured antenna patterns into channel models

Spatial channel models can be described using either a geometric (sum of sinusoids) approach or using a correlation-based approach. DUT antenna patterns can be convolved with these two descriptions in different approaches.

Geometry-based modelling of the radio channel enables separation of propagation parameters and antennas properties. The time variant impulse response matrix of the $U \times S$ (with S and U the number of transmit and receive antenna, respectively) MIMO channel is given in as:

$$\mathbf{H}(t;\tau) = \sum_{n=1}^{N} \mathbf{H}_n(t;\tau), \tag{1.8}$$

where t is time, τ is delay, N is the number of clusters, and n is cluster index. Equation 1.8 uses 2D geometry-based model implementation (only considering the angle spread in azimuth direction) to demonstrate how the antenna pattern is introduced in the channel model emulation. The impulse response matrix, composing Tx antenna array response matrices F_{tx}, Rx antenna array response matrices F_{rx} respectively, and

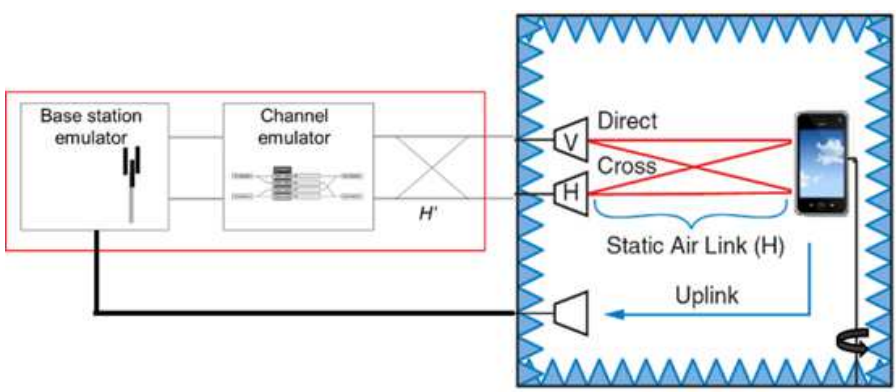

Figure 1.4: Radiated second stage throughput test.

the channel from Tx antenna element s to Rx element u for cluster n is expressed as:

$$H_{u,s,n}(t;\tau) = \sum_{m=1}^{M} \begin{bmatrix} F_{rx,u,V}(\phi_{n,m}) \\ F_{rx,u,H}(\phi_{n,m}) \end{bmatrix}^T \begin{bmatrix} \alpha_{n,m,VV} & \alpha_{n,m,VH} \\ \alpha_{n,m,HV} & \alpha_{n,m,HH} \end{bmatrix} \begin{bmatrix} F_{tx,u,V}(\phi_{n,m}) \\ F_{tx,u,H}(\phi_{n,m}) \end{bmatrix} \times \exp(j2\pi\lambda_0^{-1}(\bar{\phi}_{n,m} \cdot \bar{r}_{rx,u})) \exp(j2\pi\lambda_0^{-1}(\bar{\varphi}_{n,m} \cdot \bar{r}_{tx,u})) \times \exp(j2\pi\nu_{n,m}t)\delta(\tau - \tau_{n,m}), \quad (1.9)$$

where $F_{rx,u,V}$ and $F_{rx,u,H}$ are the antenna element u field patterns for vertical and horizontal polarizations respectively, $\alpha_{n,m,VV}$, $\alpha_{n,m,VH}$, $\alpha_{n,m,HV}$ and $\alpha_{n,m,HH}$ are the complex gains of vertical-to-vertical, vertical-to-horizontal, horizontal-to-vertical and horizontal-to-vertical polarizations of ray n, m respectively, λ is the wave length of the carrier frequency, $\bar{\phi}_{n,m}$ is the AoD unit vector, $\bar{\varphi}_{n,m}$ is the AoA unit vector, $\bar{r}_{tx,u}$ and $\bar{r}_{rx,u}$ are the location vectors of element s and u respectively, and $\nu_{n,m}$ is the Doppler frequency component of ray n, m. For the RTS method, $F_{rx,u,V}$ and $F_{rx,u,H}$ are the measured UE receiver antenna patterns from the first stage, and $F_{tx,u,V}$ and $F_{rx,u,H}$ are the predefined patterns for the base station. In the second-stage throughput test, the channel emulator rotates the antenna pattern data in Equation 1.9 against the channel model which is the same as physically rotating the device against the fixed probes in the MPAC method. For correlation-based channel model MIMO channel correlation and power imbalance property are introduced by explicitly multiplexing the corresponding covariance matrix on the independent MIMO channel coefficients. This covariance matrix can be discomposed to correlation matrix and power imbalance matrix, which is determined by the Tx, Rx antenna patterns and the specified channel model. How to derive the covariance matrix for arbitrary antenna patterns under multipath channel conditions can refer to [34]. Both geometry-based and correlation-based models are accepted in [23] for MIMO OTA test.

1.3.3 Wireless cable principle in RTS

To achieve the wireless cable connection in second stage it is necessary to measure the propagation conditions inside the anechoic chamber and modify the transmitted signals in such a way to remove the crosstalk between probe antennas and DUT antennas.

To simplify the expression a 2×2 MIMO configuration is illustrated to show how the wireless cable principle works. Assume x_1 and x_2 are the transmitted signals from the Base Station emulator, after applying the desired multipath fading channel and convolving with the complex antenna pattern we get: $f(x_1)$ and $f(x_2)$. Without signal conditioning, the first spatial stream $f(x_1)$ transmitted from probe antenna #1 will be received by both DUT antennas. Similarly, the second stream $f(x_2)$ transmitted from probe antenna #2 will also be received by both receivers. In order to create the desired situation where $f(x_1)$ is received only by receiver #1 and $f(x_2)$ is received only by receiver #2, it is necessary to calculate the transmission properties of the anechoic chamber then compute the inverse transmission matrix and multi-

ply this by the two streams. Assume the radiated channel matrix between the probe antennas and the device antennas is

$$\mathbf{H} = \begin{pmatrix} h_{11} & h_{12} \\ h_{21} & h_{22} \end{pmatrix}, \tag{1.10}$$

This channel matrix is composed of the probe antenna patterns, the signal propagation path in the anechoic chamber and the DUT receive antenna patterns. The inverse of the radiated channel matrix can be tuned in different ways as

$$\mathbf{H} = \begin{pmatrix} \alpha & \beta \\ \gamma & \delta \end{pmatrix}, \tag{1.11}$$

After applying the inverse of the radiated channel matrix to $f(x_1)$ and $f(x_2)$, the signal received at the device antennas is the same as in the cable-conducted method being:

$$\begin{pmatrix} y_1 \\ y_2 \end{pmatrix} = \begin{pmatrix} h_{11} & h_{12} \\ h_{21} & h_{22} \end{pmatrix} \begin{pmatrix} \alpha & \beta \\ \gamma & \delta \end{pmatrix} \begin{pmatrix} f(x_1) \\ f(x_2) \end{pmatrix} = \begin{pmatrix} 1 & 0 \\ 0 & 1 \end{pmatrix} \begin{pmatrix} \alpha & \beta \\ \gamma & \delta \end{pmatrix} \begin{pmatrix} f(x_1) \\ f(x_2) \end{pmatrix}. \tag{1.12}$$

The process works as both probes transmit copies of $f(x_1)$ and $f(x_2)$ at different amplitudes and phases such that $f(x_1)$ is received only at receiver #1 and $f(x_2)$ is received only at receiver #2. The process to achieve this is very similar to the precoding used to optimize signal reception for spatial multiplexing MIMO gain, while the difference is no pre-defined precoding matrix is available, the inverse matrix of propagation matrix is calculated as the precoding matrix for each test case, and this precoding matrix needs be applied after the channel model implementation.

This precoding process is not exact so the ideal situation of complete isolation between the signals and receivers is not possible. In the real test case, the received signals look like there is some signal coupling between two branches as Equation 1.13

$$\begin{pmatrix} y_1 \\ y_2 \end{pmatrix} = \begin{pmatrix} 1 & \rho \\ \rho & 1 \end{pmatrix} \begin{pmatrix} f(x_1) \\ f(x_2) \end{pmatrix} = \begin{pmatrix} f(x_1) + \rho f(x_2) \\ \rho f(x_1) + f(x_2) \end{pmatrix}. \tag{1.13}$$

Define the power ratio between the desired signal and un-desired signal as the isolation level $20\log 10(1/\rho)$ in dB, low level isolation (for example lower than 10 dB) will increase the received signals correlation level, which may bring the throughput performance degradation. However, measurements have shown that above 15 dB isolation is achievable for most devices, and this is sufficient isolation not to impact the throughput test results [28].

It should be noted that not arbitrary radiated channel matrix in Equation (1.10) is proper to be used to generate wireless cable effect because of ill-conditioned property. With the measured antenna pattern information the radiated channel matrixes can be constructed and analysed with condition number and propagation loss for all orientations, the high isolation can be achieved is optimized by selecting DUT orientations with smaller condition number and propagation loss.

1.3.4 RTS solution for 4G/5G system

The key instruments required for MIMO OTA test system is Base Station emulator and channel emulator. Below Figure 1.5 shows one RTS solution setup using Keysight BS emulator UXM7515B and channel emulator Propsim, which can support both 4G LTE and 5G NR MIMO OTA test. UXM7515B can support flexible signal format configuration, while all kinds of standardized and user-defined channel models can be emulated by Propsim including options of inverse matrix implementation and device orientation rotation in electrical way required by RTS method.

Except for MIMO OTA performance test, wireless cable method is also approved in 3GPP TR38.810 for FR2 5G NR UE Demod and Channel State Information (CSI) characteristic testing under a virtually cabled scenario. For FR2 Demod test the first stage antenna pattern measurement is skipped, but the wireless cable principle of second stage of RTS is applied without including DUTs real antenna pattern into the channel model emulation and the throughput performance evaluation. The system setup in Figure 1.5 still can work by adding radio heads to match to proper frequencies.

One possible challenge for wireless cable solution is because standard UE antenna models are used in channel model generation instead of measured patterns, no available information can be utilized to optimize the orientation selection for inverse matrix tuning, using probe antennas with orthogonal polarizations is one method to get high isolation by utilizing cross polarization ratio, but this method may face challenges for DUTs with more than two antennas.

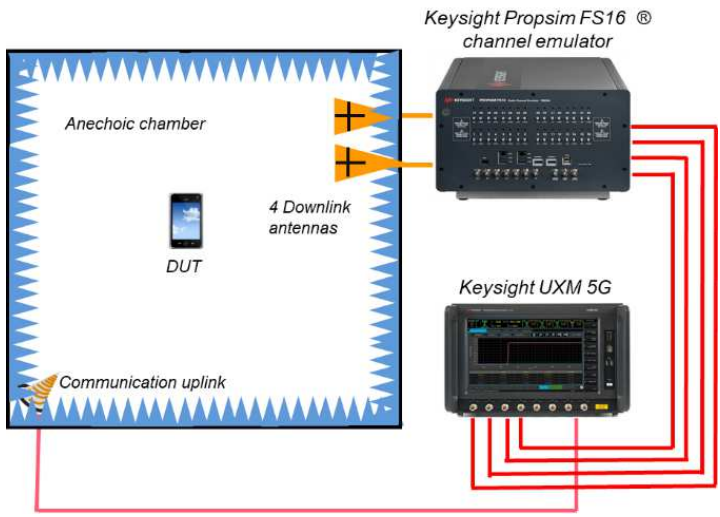

Figure 1.5: RTS MIMO OTA test setup with BS emulator and channel emulator

1.4 RF testing

The default reference testing condition for characterizing AUT radiation properties is plane wave field within the quiet zone, which is defined by the uniform amplitude and phase distribution over the AUT. Plane wave condition is required to accurately measure the AUT radiation characteristics (e.g. main beam, null depth and sidelobe), RF receiver performance (e.g. sensitivity level, and dynamic range), RF transmit performance (e.g. transmit power, signal quality, unwanted emissions), electromagnetic-susceptibility testing, scattering measurement in radar cross section (RCS), antenna array calibration and array faulty mode diagnosis, etc.

However, ideal plane wave condition does not exist in practice, yet it can be approximated using several strategies, namely the DFF method, the CATR method, the PWG method, and the NF-FF method. The pros and cons of different approaches are well discussed in the literature, and only summarize below.

- For the DFF method, the basic idea is that a plane wave at the probe antenna can be approximated if the measurement range is no smaller than the Fraunhofer far field distance. The requirement for measurement range might lead to large anechoic chamber and introduced excessive path-loss problem, especially for large-scale DUTs and for mm-wave radios.
- The basic idea of the CATR is that a plane wave can be generated using transformation with a parabolic reflector in a much shorter distance than the DFF method. The CATR offers good dynamic range due to reduced measurement range. Furthermore, it supports wide-band operation and dual-polarized measurements. However, CATR requires dedicated attention in design, e.g. dedicated edge treatment and fabrication of smooth surface for the reflector antenna, dedicated feed antenna alignment, etc. The size of the reflector antenna is typically $1.5D$.
- The NF-FF method computes the performance metrics defined for far field by using mathematical near-field to far-field transformations. We need to sample the phase and amplitude of the electrical field in the near-region over a surface, satisfying Nyquist sampling theorem. The measurement range can be rather small (e.g. typically $3\lambda - 5\lambda$ in planar near field measurement). However, there are many drawbacks of the method. First, both phase and amplitude measurements are needed for the near-field measurement. The measurement time might be massive due to sampling requirement. It is required that antenna feed port should be accessible with a signal fed to the antenna that is used as phase reference; Therefore, it might not support phase-less measurement. Furthermore, the supported RF signal is a continuous wave (CW) signal, while modulated signal 5G NR signal might not be supported.
- PWG can also enable OTA testing directly in the far-field at a reduced distance, by exciting the PWG array elements by suitably optimized complex coefficients. Compared to CATR, the PWG has several advantages, e.g. smaller measurement distance and smaller PWG aperture. It also avoids the problem of direct illumination of the quiet zone by the feed as in CATR systems. However, it is currently still not mature technology, e.g., its application to wideband and large

scale DUT is not well investigated. Furthermore, the main application has been on sub-6GHz frequency band, and few works have been reported on mm-wave bands.

The focus of this book chapter is on a recently developed mid-field OTA testing solution of 5G radios, as detailed below.

1.4.1 Mid-field solution

With the development of wireless communication systems, beamforming is one key technology adopted in 5G Base Station for both FR1 and FR2 and UE for FR2. To fully measure DUTs RF performance utilizing beamforming technology, RF testing needs to be performed by OTA. On the other hand, the joint integration of the antenna array and the RF frontend are common practice for mm-wave devices, which makes the RF connector unavailable for the RF performance test, making OTA testing the only choice.

A lot of discussions focusing on 5G NR OTA test are proceeding in 3GPP standards [35–38]. Among these 3GPP Technical Specifications (TSs) and Technical Reports (TRs), all RF metrics are defined for FF condition and FF solutions are suggested as reference for both BS and UE testing, including DFF and Indirect Far Field (IFF), which is also known as compact antenna test range (CATR). To satisfy the required test distance criteria the chamber size for DFF will be very large and high propagation loss makes the measurement of signal with low power density is impossible. CATR has a more compact test distance compared with DFF, but in order to generate enough test zone to accommodate large device the required distance between feed probe antenna and reflector also makes CATR systems facing large path loss issue.

For above reasons, it is often desirable to do OTA measurement in a distance that is much shorter than the Fraunhofer distance but can still get the far-field RF parametric results. Although NF-FF transformation is well accepted as a reliable technique to measure far-field patterns, but it requires the whole near-field phase and amplitude contributions data to derive the far-field patterns, which means that even the far-field result on one direction can only be got after the surface scanning is finished. This test method is test time prohibitive for Equivalent Isotropic Radiated power (EIRP) based test cases and currently not applicable to Effective Isotropic Sensitivity (EIS).

To overcome above test challenges a Middle-field (MF) test method is proposed with asymptotic expansion transform, and prototype test systems are developed in [39–41] to achieve OTA RF measurement with compact size. The MF testing method can reduce the test distance to $1/8$ of the Fraunhofer distance, and the MF transformation proposed for this method is significantly less complex than the traditional NFTF. The transformation does not require phase information and 3D scan for EIRP and EIS based test cases but use measured power results on two different radiated near field test distances to extrapolate the FF results.

1.4.2 MF measurement distance

The well-known Far-field (FF) Fraunhofer distance is defined as:

$$R = \frac{2D^2}{\lambda} \tag{1.14}$$

where D is the largest dimension of the AUT, and λ is the wavelength. Due to the dimensions of the massive MIMO array utilized in 5G NR, the FF requirements require a very large test distance and thus a very large OTA chamber. A MF test method is proposed to achieve accurate OTA RF measurement with compact size. This section will focus on the MF test method with known antenna array center positioning, but antenna array scale and beamforming weights information are not required for this method.

By assuming DUTs utilize antenna arrays and MF measurement distances are well in the FF of the single-element antennas, the overall antenna arrays radiation pattern respected to test distance d can be constructed using the following formula as linear superposition:

$$y(\theta,\phi,d) = \sum_{k=1}^{N} x_k G_k(\theta_k,\phi_k)\frac{\lambda d}{4\pi d_k}\exp(j2\pi\frac{d_k}{\lambda})G_P(\alpha_k,\beta_k) \tag{1.15}$$

where (θ,ϕ) are the azimuth and elevation angles of the probe antennas relative to the AUT phase center, d is the distance between the probe antenna and the AUT phase center (please note d and the following d_k are different variables), k is the index for the antenna element k, N is the number of antenna elements, x_k is the beamforming weight for antenna element k, G_k is the Far-field complex antenna pattern for antenna element k, (θ_k,ϕ_k) are the azimuth and elevation angles of antenna element k with respect to the probe antenna, λ is the wavelength, d_k is the distance between antenna element k and the probe antenna, G_P is the FF complex antenna pattern for the probe antenna, (α_k,β_k) are the azimuth and elevation angles of the probe antenna with respect to the antenna element k, $\lambda/(4\pi d_k)$ is the path loss, and $2\pi d_k/\lambda$ is the phase variation at distance d_k. Using the mathematic model in Equation 1.15 the antenna arrays patterns can be calculated at different test distances. Figure 1.7 shows the antenna gain patterns normalized by test distance d for a sample 2×8 antenna

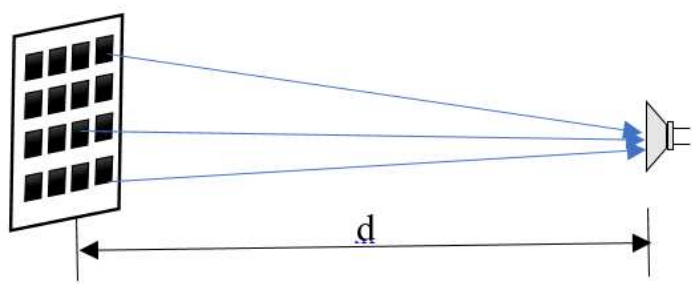

Figure 1.6: Antenna array measurement in mid-field (Fig. 1 in [41]).

array with lambda/2 as the antenna element separation. The pattern shape of traditional FF test distance (blue line) is selected as the reference, by shortening the test distance to $1/3$, $1/5$, $1/8$, $1/10$, $1/12$ and $1/15$ of FF distance, we can observe the

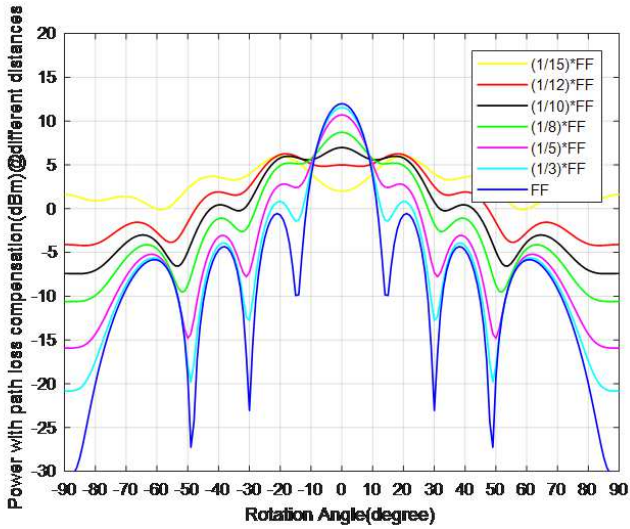

Figure 1.7: Beam gain pattern at different angels and different distances (Fig. 1 in [42]).

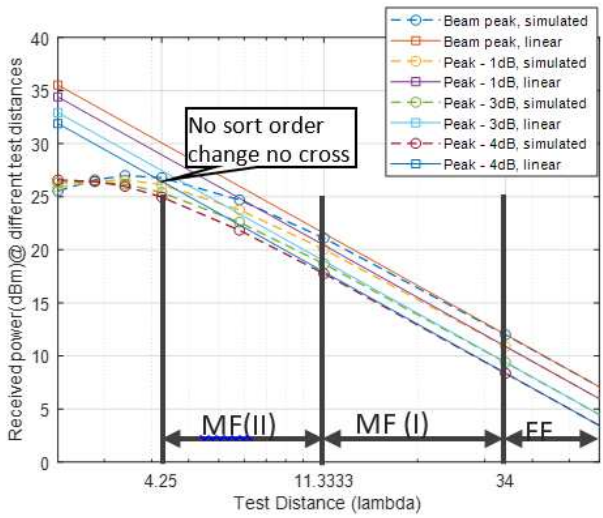

Figure 1.8: Received power at different directions within 4dB beam width w.r.t test distance (Fig. 2 in [42]).

pattern shapes change tendency. It is noticed that with a reasonable distance, for example larger than $1/8$ of FF, even though the FF antenna pattern is not fully formed, the antenna patterns main lobe shape is very similar to that of the antenna pattern in FF.

Further simulation results on the relationship of the received power with respect to the test distance and the probe antenna location direction within the 4-dB beam width are shown in Figure 1.8. The spatial intervals corresponding to the 4-dB beam width of the main lobe are shown in Figure 1.8 by four selected angles: the beam peak direction and directions which are 1-, 3-, and 4-dB gain lower than the peak direction, respectively. The power variation at different measurement distances is simulated using Equation 1.15 with dashed lines. The solid lines in Figure 1.8 are reference lines that the power changes linearly using FF assumption. For this assumed antenna array the traditional FF test distance is around 34 lambdas, in the FF region there is no difference between results followed FF theory and simulated results using Equation 1.15. In region MF (I) of larger than $1/3$ of FF, the power offset between the solid lines and dash lines is less than 0.5 dB for all directions within the 4-dB beam width. In region MF (II) of larger than $1/8$ of FF, the beam direction is still the same as that in FF, and the main lobe has a similar shape to that of FF with no sort order change and no cross, but the offset between the solid lines and dash lines is larger than 0.5 dB. Regions MF (I) and MF (II) of larger than $1/8$ of FF are suggested for the new MF OTA test system, and MF-to-FF transformation is used to derive correct FF results.

1.4.3 Basic principle for MF test method

Given the observation outlined in the previous section, near-field testing would require a transform of some sort, not necessarily a NF-FF transform utilizing a 3D scan in the vicinity of the DUT. In this section, we are outlining our basic principle for MF methodology utilizing a MF transform which allows highly accurate EIRP/EIS measurements in the near field.

The power pattern $P(\theta,\phi,d)$ of the array at test distance d can be further written as:

$$P(\theta,\phi,d) = |y(\theta,\phi,d)|^2 \tag{1.16}$$

By putting Equation (1.15) into Equation (1.16), it turns out that for arbitrary specified orientation (θ,ϕ), the gradient of power P can be simplified as a function of variable d with unknown coefficient a.

$$\frac{\partial p}{\partial d} = ad^{-2} + \Delta(d) \tag{1.17}$$

where d is the measurement distance, a is a coefficient of expansion to be determined depending on (θ,ϕ,d), and $\Delta(d)$ is a redundant term consisting of terms having a lower order than $d^(-2)$, which can be ignored. Measurement results at two different MF distances in the same direction are sufficient to accurately estimate coefficient

a. With the estimated coefficient a, the EIRP of the DUT at an arbitrary far-field distance d_f from the DUT may be determined according to

$$EIRP(d_f) = EIRP(d_1) + \int_{d_1}^{d_f} \frac{\partial p}{\partial d} d\Delta d \tag{1.18}$$

where $EIRP(d_1)$ is the measured EIRP with the probe antenna at first test distance d_1, $\frac{\partial p}{\partial d}$ is the derivation of power P to distance d, and $d\Delta d$ is the differentiation of the distance d.

The above analysis is for the transmitter antenna array EIRP measurement. For the receiver antenna array EIS measurement, similar process can be followed. By measuring the power P required to achieve the given BLER at two different distances d_1 and d_2 ($d_1 < d_2$), the unknown coefficient of expansion can be determined, then the power needed to achieve the same BLER for far field can be derived. Based on the above analysis for EIRP and EIS measurement approach, MF measurements at two different distances are needed to derive the function and the corresponding FF measurement results. With that MF concept the system implementation is designed as in Figure 1.9. It should be pointed out that this MF transform is not based on a NF to FF transformation utilizing a 3D scan of complex (magnitude and phase) fields, phase measurements of the field components are not required at all, i.e., the MF transform is based on the magnitude measurements (EIRP and EIS) only.

1.4.4 MF system and validation test

One MF OTA prototype system is setup in OTA lab shown as below Figure 1.10 can provide adjustable test range from 1m to maximum 2.5m inside a chamber with external dimension 5m×3.5m×3.5m. One CATR system with a 7m×7m parabolic reflector is selected as the reference system to provide the cross-comparison results.

The DUT used for the performance comparison is a commercial 5G NR base station in FR1. The size of the DUT is about 0.8m×0.6m, and its antenna array is about the same size. The DUTs operating frequency is around 2.6 GHz. Its far-field

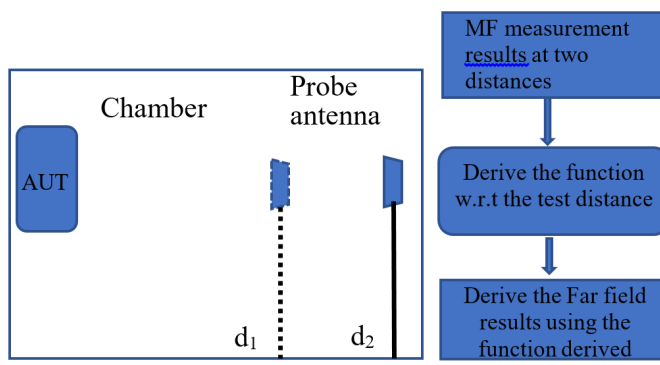

Figure 1.9: Concept and implementation of MF approach (Fig. 2 in [41]).

distance is 16.35m, and the corresponding MF distance is about 2.2m. We chose 2m and 2.5m as the two MF distance to derive the far-field results. In the comparison test, different broadcast beams and data traffic beams with different beam directions are measured. All the comparison results show that the test results in the two chambers are comparable. To save the space, only one beams measurement results are shown in Figure 1.11 as one example, more comparison results can be found in [35–37].

1.5 5G Testing Standardization

1.5.1 Performance Testing

1.5.1.1 Background

The standardization of the 5G NR has been led by 3GPP, among which the technical specification group (TSG) RAN Working Group 4 (RAN4) deals with NR MIMO OTA testing. Two frequency ranges are defined for the study, namely the FR1 covering 450 MHz to 6000 MHz and the FR2 covering 24250 MHz to 52600 MHz. Up to the RAN4 97e meeting, study items (SI) on the FR1 MIMO OTA testing have almost been accomplished, and related items about the FR2 are still under investigation. In addition, work items (WI) on MIMO OTA performance requirements for NR UEs are still on-going within 3GPP RAN4.

Performance metrics, measurement methodologies, channel models, and channel model validation procedure, are mainly defined in [24]. For FR1 MIMO OTA testing, MIMO throughput is adopted as the baseline figure of merit. Three DUT orientations, i.e., free space data mode portrait (FS DMP), free space data mode

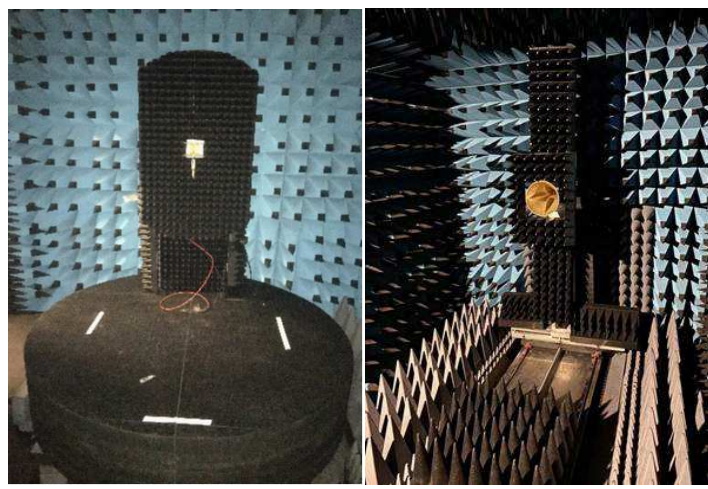

Figure 1.10: 5-axes mechanical sub-system inside the chamber. 3D rotator for DUT orientation control (left). 3-axes positioner for probe location control (right) (Fig. 8 in [41]).

landscape (FS DML), and free space data mode screen up (FS DMSU), are defined for FR1 MIMO OTA testing. For each orientation, a throughput measurement is conducted at every 30 degrees after rotating the DUT in the azimuth plane. In total, 36 measurements are collected, and the measured sensitivity values are averaged to get the final throughput result. As for measurement methodologies, MPAC and RTS test methods are adopted for FR1 MIMO OTA testing. Furthermore, 3GPP spatial channel model extended (SCME) urban micro-cell (UMi) clustered delay line A (CDL-A) and urban macro-cell (UMa) CDL-C channel models are required to be measured for FR1. In order to ensure that the channel models are correctly implemented in the quiet zone, measurements including Doppler/temporal correlation, PDP, spatial correlation, cross-polarization, and power validation, need to be validated in the test zone before the actual throughput testing.

For FR2 MIMO OTA testing, similar as FR1, MIMO throughput is adopted as the performance metric. Different from the 2D scan in the azimuth plane for FR1, a 3D scan consisting of 36 test points on a sphere is specified for FR2 MIMO OTA testing. In terms of measurement methodologies, 3D MPAC is selected for FR2 MIMO OTA testing, and the 3D channel model indoors (InO) CDL-A and UMi CDL-C are selected for testing. Regarding channel model validation, spatial correlation that is used for FR1 is replaced with PAS similarity percentage (PSP).

1.5.1.2 Measurement methodologies

For FR1, 2D MPAC and RTS test methods are adopted as the reference methods, while the 3D MPAC test method is selected in FR2.

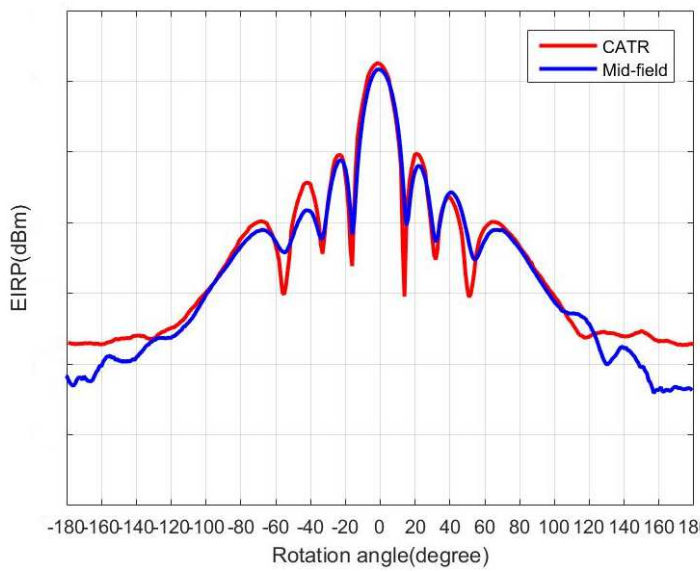

Figure 1.11: 2D antenna pattern horizontal cut comparison (traffic beam H0V19) (Fig. 9 in [41])

2*D MPAC for FR*1

2D MPAC test method is regarded as a reference for FR1 MIMO OTA testing. By utilizing multiple probes around the DUT, the spatial profile of the target channel can be produced in the test zone [7, 44]. Considering the tradeoff between the cost of CE resources and the possible desired test zone size [45], 16 uniformly spaced probes on a ring is adopted as the final probe layout in FR1 MIMO OTA testing by 3GPP RAN4 as shown in Figure 1.12 and a photo of practical setup is shown in Figure 1.13, respectively.

*RTS for FR*1

The RTS test method [46] is defined as the harmonized method for FR1 MIMO OTA testing. An example of the RTS system layout for 4×4 NR FR1 MIMO OTA testing is illustrated in Figure 1.14. The BS emulator sends downlink signals to the CE. Specified channel models are implemented in the CE, and the output signals

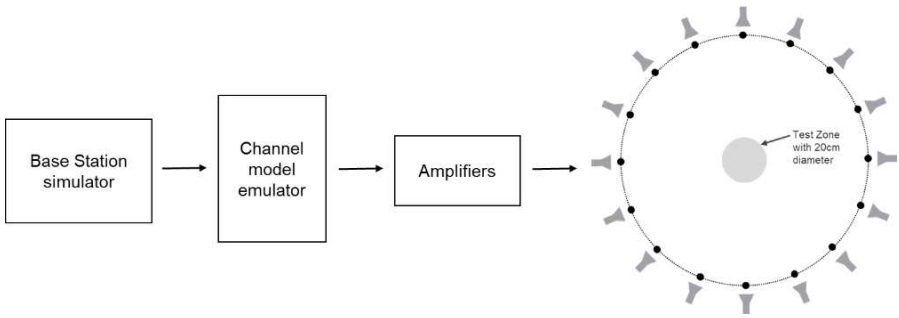

Figure 1.12: 2D MPAC system layout for NR FR1 MIMO OTA testing.

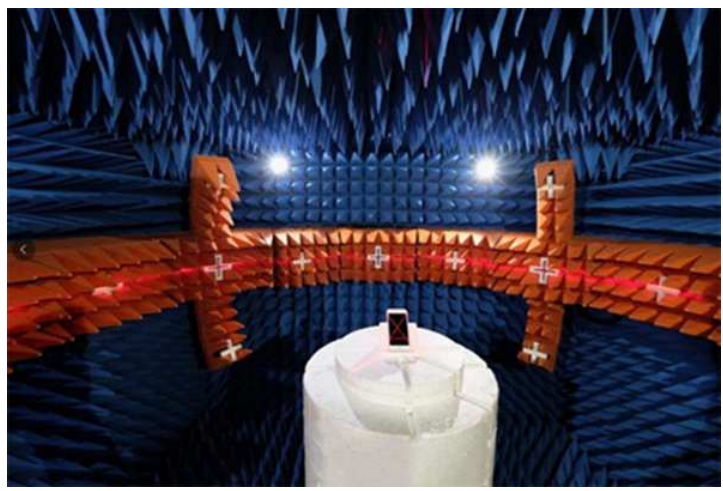

Figure 1.13: MPAC anechoic chamber for FR1 MIMO OTA testing.

from the CE are fed to the probes. The DUT is placed in the center of the anechoic chamber, and a separate communication antenna is used for the uplink connection with the BS emulator. Depending on the chamber size and path loss, amplifiers may be needed for downlink and uplink.

The first stage of RTS is to acquire the DUTs complex antenna pattern including both amplitude and phase. One way to obtain this is through the so-called antenna test function (ATF). In the second stage of RTS, the transfer function between the probes and the DUT antennas can be obtained through the ATF. A weighting matrix which is the inverse of the transfer function can be applied in the CE so that the isolation between the desired link and crosstalk link is maximized. The DUT antenna pattern measured in the first stage can be added to the emulated channel in the CE. Finally, throughput tests can be performed with different channel models.

The internal structure of the actual anechoic chamber for the RTS method is depicted in Figure 1.15. The DUT is placed in the center of the anechoic chamber and surrounded by multiple probes, and 2D or 3D antenna patterns can be measured by rotating the DUT with the ATF. During the throughput measurement, the action of physically rotating the DUT as with the MPAC method is, instead, realized by applying the resulting DUT antenna pattern that is mathematically rotated based on the measured DUT antenna pattern according to the desired angle in the CE.

The advantages and disadvantages of the MPAC and RTS methods for NR FR1 MIMO OTA testing are given in Table 1.1.

3*D MPAC for FR*2

Different methods for FR2 MIMO OTA testing have been proposed in 3GPP and discussed extensively in [47–49]. As a result, 3D MPAC [14, 50] is adopted as the final test method by 3GPP RAN4, and the system setup is illustrated in Figure 1.16. Note that due to the much higher frequency and corresponding channel models for FR2, the testing operation is different from 2D MPAC for FR1, as listed in the following aspects:

- From the perspective of system setups, amplifiers used in FR1 are replaced by radio heads with the functions of frequency conversion and power amplification.

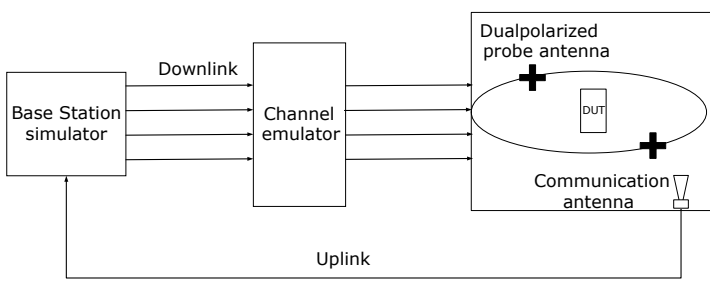

Figure 1.14: Example RTS system layout for 4×4 NR FR1 MIMO OTA testing.

- Compared with the spatial correlation used in FR1, PSP is used in FR2 to measure the similarity of the PAS produced by OTA system and the reference PAS [51].
- To emulate the behavior of the channel models in FR2, 6 dual-polarized probes are placed on a 3D sector with minimum radius of 0.75m from the center of the test zone. The exact probe locations over the channel model coordinate system are shown in [24]. The 6 probe locations are determined following the discussed probe-selection principle.
- In comparison to the 2D scan in FR1 MIMO OTA testing, 3D scan is adopted in FR2 MIMO OTA testing. 36 evenly spaced test points determined using the charged particle approach for FR2 MIMO OTA testing is listed in Table 6.2.3.2 – 1 of [24].

An exemplary environment inside the anechoic chamber for FR2 MIMO OTA testing is shown in Figure 1.17. For the channel models to be tested and the corresponding probe placement positions to be extendable in the future, a setup with

Figure 1.15: FR1 RTS anechoic chamber.

Table 1.1 Advantages and Disadvantages of MPAC and RTS in FR1 MIMO OTA testing.

Methods	Advantages	Disadvantages
MPAC	1) A real physical channel spatial profile on the DUT side is realized. 2) The same fading sequence can be reused for different DUTs under the same target channel model.	1) High setup complexity and cost. 2) Channel model validation is needed prior to throughput testing.
RTS	1) Low setup complexity and cost. 2) Capable of any arbitrary channel models.	1) DUTs need to support the ATF. 2) Only support DUTs of non-adaptive antenna patterns. 3) The weighting matrix needs to be recalculated when the DUT condition is changed.

6 dual-polarized probes being placed in the 3D sector is designed which can be moved freely, and the 2D positioner can be controlled with the software automatically. Furthermore, the addition of radio head equipment allows CEs that originally only support FR1 testing to support for FR2 as well. As an important component, both the capability and performance of the radio head need to be considered in the actual test system. The radio head needs to have stable frequency conversion and accurate power amplification to avoid distortion of the signal by the component itself. Secondly, the single-port bidirectional transmission capability can halve the number of required CE ports, while supporting bidirectional testing.

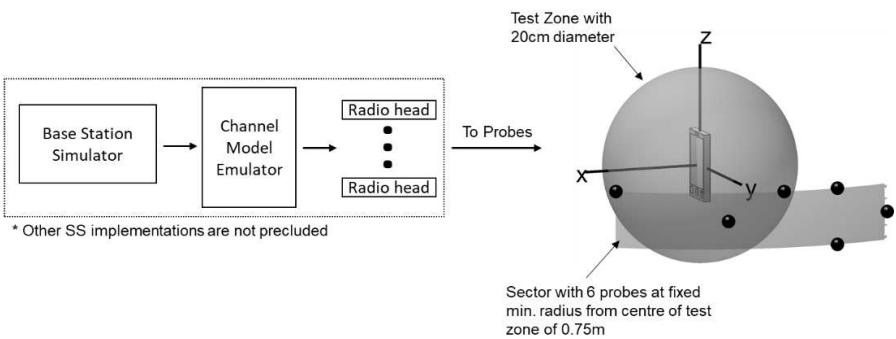

Figure 1.16: 3D MPAC system layout for NR FR2 MIMO OTA testing.

Table 1.2 Channel model validation for FR1 and FR2.

FR1	**FR2**	**Validation instrument**
Power validation		BS simulator & Spectrum analyzer
Doppler/Temporal correlation		Signal generator & Spectrum analyzer
Cross-polarization		
PDP		Vector network analyzer (VNA)
Spatial correlation	PSP	

1.5.1.3 Channel Model Validation

In order to ensure that the channel models are correctly emulated in the test zone, 3GPP RAN4 also defined the parameters and procedure of channel model validation. Table 1.2 illustrates the key performance indicators (KPI) and instruments needed to accomplish the procedure.

For FR1 MIMO OTA channel models, the same verification parameters with 4G MIMO OTA testing, i.e. PDP, Doppler/temporal correlation, spatial correlation, cross-polarization, and power validation, are adopted for the channel model validation. For FR2 MIMO OTA, PSP is used instead of the spatial correlation to validate how well the channel model is emulated compared with the target one. The validation procedures have been described in detail for different parameters in [24]. Detailed parameters for time and frequency samples have not been defined by 3GPP RAN4. Moreover, the procedure of the PSP validation in FR2 is still under discussion within 3GPP RAN4.

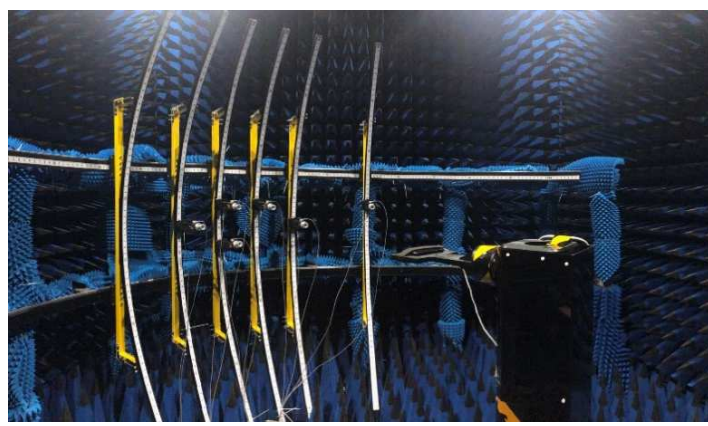

Figure 1.17: FR2 3D MPAC anechoic chamber in labs

1.5.2 RF Testing

1.5.2.1 5G NR RF BS standards

3GPP started 5G standard research in 2013, and the RF specifications for both BS and UE are discussed in the TSG RAN4. After 5 years, the first edition of 5G NR standards was frozen in 2018. For the BS, there are four major RF technical specifications (TS), i.e., BS transmission and reception characteristics [52], electromagnetic compatibility (EMC) [53], conducted conformance testing [54] and radiated conformance testing. Furthermore, three technical reports (TR) [55–57] are recommended as the supplements to the above TS. In [55], transmitter and receiver characteristics of the active antenna system (AAS) BS deployment scenarios are studied, and the EMC requirements are proposed as well. In [56], the detailed AAS BS RF OTA test methods are described, e.g., far field (FF), near field (NF), CATR, PWS, and RC.

The test cases can be divided into two parts, i.e. transmitter characteristics and receiver characteristics:

- Transmitter test cases can be summarized as three categories. The first is the power class test, e.g., TRP and effective isotropic radiated power (EIRP). The second is the radiated signal quality test, e.g., error vector magnitude (EVM), frequency error and time alignment. The third is the radiated unwanted signal test, including unwanted emission and intermodulation. These cases above measure the BS coverage ability and transmission signal quality.
- Receiver test cases can be divided into four kinds. The first is the OTA receiver power ability test cases, e.g., sensitivity, reference sensitivity level, and dynamic range. The second is the in-band and out-band blocking test cases. The third is the unwanted signal test cases including spurious emission and intermodulation. The last is the in-channel selectivity. These test cases verify the BS receive signals quality and anti-interference performance.

The basic specifications and capabilities of BS are given in Table 1.3 and Table 1.4. The general commercial macro-BS specifications are shown in Table 1.3, which are based on the BS manufacture's declaration.

As shown in Table 1.3, the number of antenna elements of the FR2 case is significantly larger than that of the FR1, whereas the physical size of the BS is smaller. When the frequency increases, the antenna element can be designed to be smaller, thus the millimeter wave base station can accommodate more antenna elements. Moreover, the FR2 BS has a larger working bandwidth than the FR1 BS. In addition, the beam coverage of FR1 BS and FR2 BS are almost the same except it goes up to $+6^\circ$ in the vertical direction in FR1 and $+17^\circ$ in FR2.

As shown in Table 1.4, the output power of FR1 BSs is much higher than that of FR2 BSs, because the power amplifier has a better performance at the low frequency. Since the array aperture of FR2 BSs in electric size is much bigger than that of FR1 BSs, the beam width of FR2 BS is smaller.

Traditional OTA test methods, e.g., far field, CATR, has been widely used. These test systems are usually large, heavy, and costly for BS measurement. To cope with that, the plane wave synthesizer (PWS) method was developed in 2018 and ap-

Table 1.3 5G NR BS basic specifications.

Specifications	**FR1 5G NR BS**	**FR2 5G NR BS**
Typical size	About 1m×0.5m×0.3m	About 0.5m×0.3m×0.25m
Frequency band	2.6 GHz, 3.5 GHz, 4.9 GHz	26 GHz, 28 GHz, 39 GHz
Working bandwidth	100 MHz	400 MHz
Duplex mode	TDD	TDD
Number of RF channels	8 Tx/8 Rx, 4 Tx/4 Rx	4 Tx/4 Rx, 2 Tx/2 Rx
Number of antenna elements	At least 96	512/1024
Beam coverage	Horizontal maximum $\pm 60^\circ$ Vertical $+6^\circ$ to -17°	Horizontal maximum $\pm 60^\circ$ Vertical maximum $\pm 17^\circ$

Table 1.4 5G NR BS typical radiated capabilities.

Specifications	**FR1 5G NR BS**	**FR2 5G NR BS**
Test cases	FR1 5G NR BS	FR2 5G NR BS
Output power	≥ 53 dBm	≥ 30 dBm
Maximum EIRP	≥ 76 dBm	≥ 60 dBm
Antenna gain	≥ 23 dBi	≥ 30 dBi
Occupied bandwidth	≤ 100 MHz	≤ 400 MHz
EVM (64QAM)	$\leq 8\%$	$< 9\%$
Receiver sensitivity	≤ -116 dBm	≤ -113 dBm
Unwanted emissions	Meet the requirements	≤ -39 dBW/200 MHz

proved as a BS test method in 2019 by 3GPP. Compared with the CATR test system, the PWS test system requires a smaller chamber size, and the weight is lighter. A practical PWS system is shown in Figure 1.18. The typical size of a PWS system is 6m×4m×4m for the FR1 BS measurement, and it can provide at least a test quiet zone of 1m×1m.

It is noted that the measurement time is very important. At present, many OTA test cases are performed by directly sampling on the entire spherical surface, e.g., the equal angle spherical acquisition method for TRP measurements. For example, in FR1 BS TRP testing, when the sampling interval is 6 degrees, a total of 1801 points on the 4π solid angle needs to be measured. As the sampling interval decreases with the increase of the frequency, more data need to be collected in FR2 TRP testing. In order to save time, a few other data acquisition methods have been included in [54], e.g., the wave vector space, the two-cut method and the three-cut method. However, it may deteriorate in the test accuracy.

The RC test method is adopted in [56] for the BS OTA testing. In some laboratories, as illustrated in Figure 1.19. Reverberation chamber, the RC test method is performed for FR2 BSs TRP testing. The difference of the TRP test value be-

tween CATR and RC is only about 0.3 dB, but the test time of RC is hundreds of

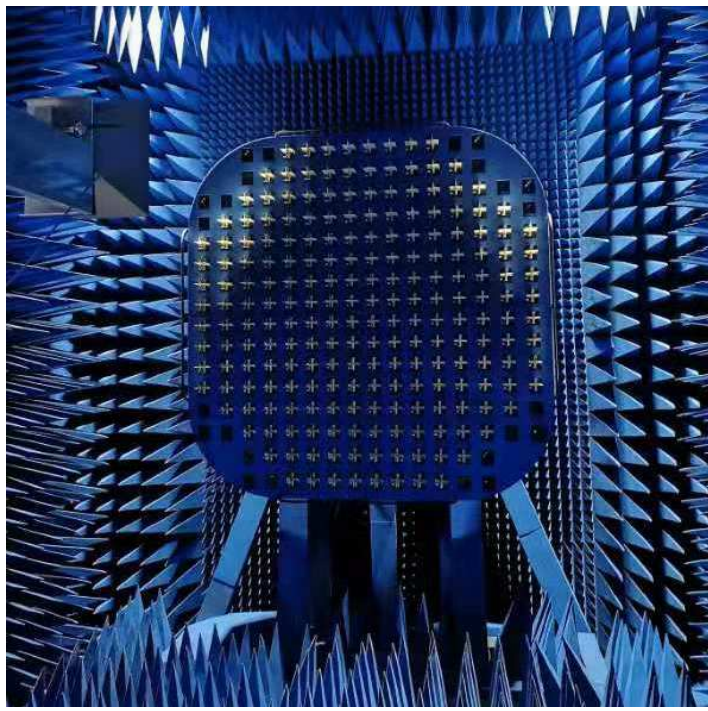

Figure 1.18: Plane wave synthesizer.

Figure 1.19: Reverberation chamber.

times lower than that of CATR. Moreover, the chamber size of the RC is only about 1.5m×1.5m×2m, and the cost of an RC test system is about one third of the CATR test system. The RC test method can also be used for some testing items in FR1 BS testing.

1.5.2.2 5G NR RF UE standards

The standards of 5G NR UE mainly include protocol conformance specifications, radio resource management (RRM) conformance specifications, radio transmission and reception conformance specifications. The protocol conformance test requirement is introduced in [58], which specifies protocol stack development verification requirements. The RRM conformance test requirement is studied in [59], which specifies mobility management and performance testing requirements. The RF conformance test requirement is studied in [60], which specifies the transmitter and receiver requirement.

UE RF standards mainly include the technical requirement, test procedure, and test method. The RF technical specifications of FR1 devices and FR2 devices are introduced in [60] and [61] respectively, which specify the minimum RF transmission and reception requirements of standalone (SA) devices. The technical specification for FR1 and FR2 interworking operation with other radios is introduced in [62], which specifies the minimum RF transmission and reception requirements of NSA devices. The UE RF conformance specifications for FR1 and FR2 devices are introduced in [63] and [64] respectively, which specify the RF measurement procedures of the conformance testing. Moreover, the RF conformance specification for FR1 and FR2 interworking operation with other radios is introduced in [65], which specifies the measurement procedures of the conformance testing for carrier aggregation between FR1 and FR2, and additional requirements due to the NR NSA operation mode with evolved universal terrestrial radio access (E-UTRA). Besides, the test method for FR2 is studied in [66], which details the OTA test methodology, the associated measurement uncertainty budget, and the related test tolerance. FR1 devices are measured through conducted methods and FR2 devices are measured through OTA methods. The enhanced test method for FR2 UE is introduced in [67], which enhances the FR2 RF testing methodology and quantifies the impact of the enhancement on the measured UE performance, as related to the polarization basis mismatch between the test equipment and UE. Moreover, it also adds support for testing under extreme temperature conditions.

In the 5G FR1 frequency band, the characterization of RF performance is evaluated through cabled connections at the temporary antenna connectors. This bypasses the devices antenna. In the 5G FR2 millimeter wave frequency band, however, RF units and antenna interfaces cannot be separated, and hence all the RF characteristics have to be tested through the OTA test method.

RF test cases are studied in the following three aspects: transmitter (Tx) and receiver (Rx) in-band test cases, Tx and Rx spurious test cases, and Rx blocking test cases. Tx and Rx in-band test cases mainly include the power class test, modulation and demodulation test, and adjacent channel leakage power test, e.g. EIRP, TRP, EIS, error vector magnitude (EVM), and frequency error. EIRP and TRP are the two

key technical indicators to measure the power class of the device under test. A very high EIRP or TRP may cause interference to other frequency bands and systems. On the other hand, a low EIRP or TRP may decrease the coverage. In [64], the EIRP value of FR2 UE with power level 3 in band n258 is limited between 22.4 dBm and 43 dBm, and the maximum TRP value is less than 23 dBm. EIS is a key technical parameter of receiver performance test, which measures the minimum power with which the device under test can still maintain a pre-defined throughput level averaged over different directions. The EIS affects the effective coverage of base station. The reference EIS value of FR2 UE with power level 3 supporting 100 MHz bandwidth in band n258 is set lower than -85.3 dBm in [64]. The EVM is a key technical parameter for evaluating modulation and demodulation capability of FR2 UEs, which represents the difference between the reference waveform and the measured waveform. The frequency error is to verify the accuracy of a UEs receiver and transmitter detecting and generating the correct carrier frequency with respect to the stimulus signal offered by the base station under ideal propagation conditions and low power level.

Tx and Rx spurious test cases mainly include the transmitter spurious emission (SE) and receiver SE. SEs are caused by unwanted transmitter effects, e.g. harmonics emissions, parasitic emissions, intermodulation products, and frequency conversion products. Extremely high SEs may cause interference to other frequency bands and systems, which will affect the frequency planning.

Rx blocking test cases mainly include the adjacent channel selectivity (ACS) and in-band blocking, which represent the UE's anti-interference ability. ACS tests the UEs ability to receive data with a given average throughput for a specified reference measurement channel, in the presence of an adjacent channel signal at a given frequency offset from the central frequency of the assigned channel, under conditions of ideal propagation and no added noise. In-band blocking is defined for an unwanted interfering signal falling into the UE receive band or into the spectrum equivalent to twice the channel bandwidth below or above the UE receive band at which the relative throughput shall meet or exceed the minimum requirement for the specified measurement channels.

In order to test these cases in a reliable environment, many solutions for the OTA testing are proposed in [66], including DFF, IFF, and NF. Currently, many instrument manufacturers have proposed FR2 CATR solutions for the RF conformance testing. In this chapter, an CATR chamber will be introduced as a standard IFF test system to evaluate the FR2 UEs RF performance.

The 5G NR FR2 UE RF conformance testing system is an integrated solution consisting of the CATR, combined axes UE positioner, multi-feed antenna array, link antenna, system simulator, signal analyzer, signal generator, and chamber control software, as illustrated in Figure 1.20, which could offer an effective interface for test case execution, analysis and reporting. As shown in Figure 1.20, the CATR chamber is used to form a plane wave at the UE position in which the LTE and FR2 link antenna are used to establish the call from the UE to the system simulator. Tx and Rx in-band test cases are executed by the system simulator and the combined axes UE positioner. The signal analyzer and multi-feed antenna array are used for the

Tx and Rx spurious test. The signal generator is proposed to perform the Rx blocking test. With this chamber, the RF conformance testing specified by both 3GPP and global certification forum (GCF), including beamforming in 3D space at mm-wave frequencies, predefined and customizable FR2 RF performance tests, extreme temperature and humidity condition tests, and in-band and out-of-band emission tests, can be performed efficiently. To meet the wide test frequency range and to reduce the test time in SE measurements, based on the CATR system, a multi-feed test system can be utilized, which is composed of one feed working from 24 GHz to 44 GHz, one feed working from 6 GHz to 24 GHz, one feed working from 40 GHz to 60 GHz and one feed working from 60 GHz to 90 GHz, which can meet the requirements of the SE test from 6 GHz to the second harmonic. This solution greatly reduces the test time, and multiple feeds are placed near the parabolic focus in comparison to the original single feed system. The offset feed can form a plane wave with a certain angle within the original area in the CATR, so as to realize multi-band simultaneous measurements.

To sum up, in this section, the protocol conformance specification, RRM conformance specification, and RF conformance specification of 5G NR UE are reviewed. The RF related standards are introduced in detail, including the technical specifications, test procedures and test methods. The Tx and Rx in-band test cases, SE tests and blocking test cases to evaluate the RF performance of 5G FR2 UE are discussed. A multi-feed CATR RF test chamber is proposed to execute these RF test cases with which the efficiency and dynamic range is improved through three effective methods. In the future, low-cost solutions and more efficient systems will be proposed for FR2 UE RF tests.

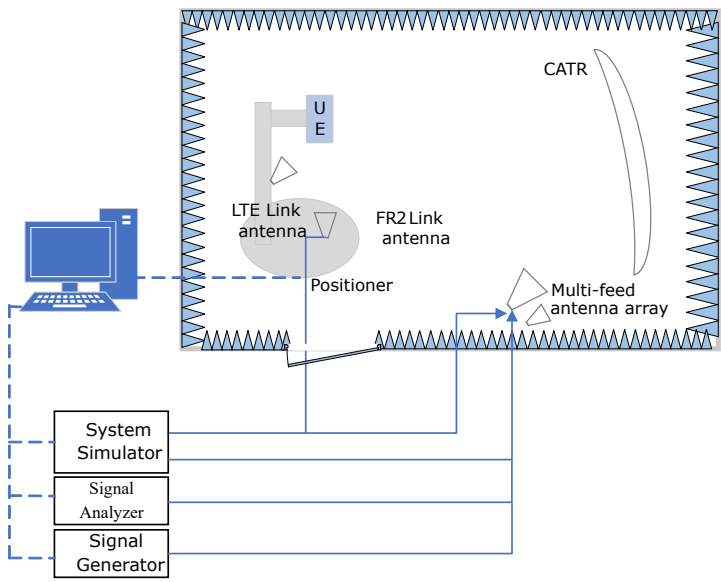

Figure 1.20: RF test system layout for 5G NR FR2 UE RF test.

1.6 Conclusion

The 5G systems promise higher spectral efficiency and energy efficiency, lower latency, and more reliable communications. These advantages are supported by mmWave and/or massive multiple-input multiple-output (M-MIMO) techniques. Cable conducted testing has been the dominant testing method for sub-6 GHz conventional communication systems, where antenna ports are mostly accessible for conducted testing. In the conducted testing, antenna characteristics are omitted completely by testing from antenna ports. However, for M-MIMO antenna systems with hundreds of antenna elements, conducted testing obviously becomes infeasible. Moreover, it is likely that mmWave systems will not have standard antenna ports, rendering OTA the only testing solution. In this book chapter, we firstly discussed the OTA solutions for the performance testing, where the objective is to evaluate 5G radio performance, e.g. throughput, under realistic spatial channel conditions. We discussed two standard OTA testing methods, namely the MPAC and RTS. The focus has been the principle, key challenges, practical systems, pros and cons of the method. As for the RF OTA testing, where the goal is to test 5G RF parameters under ideal plane wave conditions. We detailed a mid-field testing method. The principle, system requirement and capabilities are discussed. The third part introduces the current status of OTA testing of 5G radios in standardization, including both performance testing and RF testing are discussed.

Acknowledgment

The authors would like to acknowledge the help from Dr. Yilin Ji and Mr. Yejian Lyu for editing and preparation of the chapter.

References

[1] Certification C. Test plan for mobile station over the air performance, method of measurement for radiated RF power and receiver performance; 2008. Rev 2.2.2.

[2] Foegelle M. Over-the-Air Performance Testing of Wireless Devices with Multiple Antennas. RF Design. 2006 02;2012.

[3] ; Systems and methods for over the air performance testing of wireless devices with multiple antennas. ; 2012.

[4] Iwai H, Yamamoto A, Sakata T, et al. Spatial fading emulator for handset antennas. In: 2005 IEEE Antennas and Propagation Society International Symposium. vol. 1A; 2005. p. 218–221 Vol. 1A.

[5] Kyösti P, Hentilä L, Fan W, et al. On Radiated Performance Evaluation of Massive MIMO Devices in Multiprobe Anechoic Chamber OTA Setups. IEEE Transactions on Antennas and Propagation. 2018;66(10):5485–5497.

[6] Kyösti P, Nuutinen J, Kolu J, et al. Channel Modelling for Radiated Testing of MIMO Capable Terminals. In: Proc. of ICT-Mobile Summit; 2009. .

[7] Kyösti P, Jämsä T, Nuutinen J. Channel Modelling for Multiprobe Over-the-Air MIMO Testing. International Journal of Antennas and Propagation. 2012 03;2012.

[8] Kotterman WAT, Heuberger A, Thom RS. On the accuracy of synthesised wave-fields in MIMO-OTA set-ups. In: Proceedings of the 5th European Conference on Antennas and Propagation (EUCAP); 2011. p. 2560–2564.

[9] Laitinen T, Kyösti P, Nuutinen J, et al. On the number of OTA antenna elements for plane-wave synthesis in a MIMO-OTA test system involving a circular antenna array. In: Proceedings of the Fourth European Conference on Antennas and Propagation; 2010. p. 1–5.

[10] Kotterman W. Increasing the volume of test zones in anechoic chamber MIMO Over-the-Air test set-ups. In: 2012 International Symposium on Antennas and Propagation (ISAP); 2012. p. 786–789.

[11] Fan W, Carton I, Kyösti P, et al. Emulating Ray-Tracing Channels in Multiprobe Anechoic Chamber Setups for Virtual Drive Testing. IEEE Transactions on Antennas and Propagation. 2016;64(2):730–739.

[12] Fan W, Kyösti P, Fan S, et al. 3D Channel Model Emulation in a MIMO OTA Setup. In: 2013 IEEE 78th Vehicular Technology Conference (VTC Fall); 2013. p. 1–5.

[13] Kyösti P, Fan W, Pedersen GF, et al. On Dimensions of OTA Setups for Massive MIMO Base Stations Radiated Testing. IEEE Access. 2016;4:5971–5981.

[14] Kyösti P, Hentilä L, Fan W, et al. On Radiated Performance Evaluation of Massive MIMO Devices in Multiprobe Anechoic Chamber OTA Setups. IEEE Transactions on Antennas and Propagation. 2018;66(10):5485–5497.

[15] Fan W, Kyösti P, Rumney M, et al. Over-the-Air Radiated Testing of Millimeter-Wave Beam-Steerable Devices in a Cost-Effective Measurement Setup. IEEE Communications Magazine. 2018;56(7):64–71.

[16] Fan W, Carton I, Kyösti P, et al. A Step Toward 5G in 2020: Low-cost OTA performance evaluation of massive MIMO base stations. IEEE Antennas and Propagation Magazine. 2017;59(1):38–47.

[17] Ji Y, Fan W, Pedersen GF, et al. On Channel Emulation Methods in Multiprobe Anechoic Chamber Setups for Over-the-Air Testing. IEEE Transactions on Vehicular Technology. 2018;67(8):6740–6751.

[18] Fan W, Zhang F, Wang Z. Over-the-Air Testing of 5G Communication Systems: Validation of the Test Environment in Simple-Sectored Multiprobe Anechoic Chamber Setups. IEEE Antennas and Propagation Magazine. 2021;63(1):40–50.

[19] Fan W, Hentilä L, Kyösti P. Spatial Fading Channel Emulation for Over-the-air Testing of mmWave Radios: Concepts and Experimental Validations. Frontiers of Informaion Technology & Electronic Engineering. 2021;.

[20] R4-091361. MIMO OTA test methodology proposal. Agilent Technologies, 3GPP TSG-RAN WG4 Meeting #bis; 2009. Rev 2.2.2.

[21] Jing Y, Zhao X, Kong H, et al. Two-stage over-the-air (OTA) test method for LTE MIMO device performance evaluation. International Journal of Antennas and Propagation. 2012 07;2012.

[22] R4-66AH-0012. Incorporating self-interference into the two-stage method. Agilent Technologies, Tri-L Solutions, 3GPP RAN4#66AH; 2013. Rev 2.2.2.

[23] 977 T. Verification of radiated multi-antenna reception performance of User Equipment (UE). V14.5.0; 2018.

[24] 827 T. Study on radiated metrics and test methodology for the verification of multi-antenna reception performance of NR User Equipment (UE),. V1.3.1; 2020.

[25] Certification C. Test Methodology. ,MIMO Radiated Two Stage; 2020.

[26] Rumney M, Kong H, Jing Y. Practical active antenna evaluation using the two-stage MIMO OTA measurement method. In: The 8th European Conference on Antennas and Propagation (EuCAP 2014); 2014. p. 3500–3503.

[27] Jing Y, Kong H, Rumney M. MIMO OTA test for a mobile station performance evaluation. IEEE Instrumentation Measurement Magazine. 2016;19(3):43–50.

[28] Rumney M, Hongwei Kong, Ya Jing, et al. Recent advances in the radiated two-stage MIMO OTA test method and its value for antenna design optimization. In: 2016 10th European Conference on Antennas and Propagation (EuCAP); 2016. p. 1–5.

[29] Jing Y, Hertel T, Kong H, et al. Recent Developments in Radiated Two-Stage MIMO OTA Test Method. In: 2020 14th European Conference on Antennas and Propagation (EuCAP); 2020. p. 1–5.

[30] 978 T. E-UTRA UE Antenna test function definition for two-stage MIMO OTA test method. v13.0.0, 3GPP;.

[31] Jing Y, Kong H, Rumney M. MIMO OTA test for a mobile station performance evaluation. IEEE Instrumentation Measurement Magazine. 2016;19(3):43–50.

[32] Fan W, Kyösti P, Hentilä L, et al. MIMO Terminal Performance Evaluation With a Novel Wireless Cable Method. IEEE Transactions on Antennas and Propagation. 2017;65(9):4803–4814.

[33] Zhang F, Fan W, Wang Z. Achieving Wireless Cable Testing of High-Order MIMO Devices With a Novel Closed-Form Calibration Method. IEEE Transactions on Antennas and Propagation. 2021;69(1):478–487.

[34] Dao M, Nguyen V, Im Y, et al. 3D Polarized Channel Modeling and Performance Comparison of MIMO Antenna Configurations With Different Polarizations. IEEE Transactions on Antennas and Propagation. 2011;59(7):2672–2682.

[35] NR. Base Station (BS) Conformance Testing Part 2: Radiated Conformance Testing (Release 15). 3GPP TS 38141-2. 2018;.

[36] NR. User Equipment (UE) radio transmission and reception. 3GPP TS 38521 v1640. 2020;.

[37] NR. User Equipment (UE) conformance specification; Radio transmission and reception. 3GPP TS 38521 v1640. 2020;.

[38] NR. Study on test methods. 3GPP TR 38810 v1650. 2019;.

[39] Kong H, Wen Z, Jing Y, et al. A compact millimeter wave (mmWave) midfield over the air (OTA) RF performance test system for 5G massive MIMO devices. In: 2018 IEEE MTT-S International Wireless Symposium (IWS); 2018. p. 1–4.

[40] Kong H, Wen Z, Jing Y, et al. Midfield Over-the-Air Test: A New OTA RF Performance Test Method for 5G Massive MIMO Devices. IEEE Transactions on Microwave Theory and Techniques. 2019;67(7):2873–2883.

[41] Kong H, Jing Y, Wen Z, et al. Mid-field OTA RF test method: new developments and performance comparison with the compact antenna test range (CATR). In: 2020 14th European Conference on Antennas and Propagation (EuCAP); 2020. p. 1–5.

[42] Jing Y, Wen Z, Hertel T, et al. Near Field Test Methodology for 5G UE FR2 Radiated Performance Measurements. In: 2021 15th European Conference on Antennas and Propagation (EuCAP); 2021. p. 1–5.

[43] R4-2016213. On Test methodology for high DL power and low UL power test cases. 3GPP TSG-RAN WG4 Meeting #97-e. 2020;.

[44] Fan W, Carreo Bautista de Lisbona XCB, Sun F, et al. Emulating Spatial Characteristics of MIMO Channels for OTA Testing. IEEE Transactions on Antennas and Propagation. 2013;61(8):4306–4314.

[45] R4-1910809. Further discussion on NR FR1 MPAC Probes Layout. VIVO, 3GPP RAN4 #92bis. 2019;.

[46] Shen P, Qi Y, Yu W, et al. Notice of Retraction: Inverse Matrix Auto-Search Technique for the RTS MIMO OTA TestPart 1: Theory. IEEE Transactions on Electromagnetic Compatibility. 2017;59(6):1716–1723.

[47] NR. User Equipment (UE) conformance specification; Radio transmission and reception. 3GPP TS 38521 v1640. 2020;.

[48] R4-1711501. Further analysis of RTS applicability to BS demodulation performance testing. Keysight Technologies, 3GPP RAN4 #84bis. 2017;.

[49] R4-170669. SS MPAC for RRM/Demod. Keysight, RAN4 AH#2. 2017;.

[50] Fan W, Zhang F, Wang Z. Over-the-Air Testing of 5G Communication Systems: Validation of the Test Environment in Simple-Sectored Multiprobe Anechoic Chamber Setups. IEEE Antennas and Propagation Magazine. 2021;63(1):40–50.

[51] R4-1705831. Metrics for evaluating RRM/Demodulation Measurement Setup. Keysight, RAN4 #83. 2017;.

[52] NR. Base Station (BS) radio transmission and reception. 3GPP TS 38104, Tech Spec Rel 16, V1650. 2020;.

[53] NR. Base Station (BS) ElectroMagnetic Compatibility (EMC). 3GPP TS 38113, Tech Spec Rel 16, V1650. 2020;.

[54] NR. Base Station (BS) conformance testing; Part 1: Conducted conformance testing. 3GPP TS 38141-1, Tech Spec Rel 16, V1650. 2020;.

[55] Study of Radio Frequency (RF) and Electromagnetic Compatibility (EMC) requirements for Active Antenna Array System (AAS) base station. 3GPP TR 37840, Tech Repo Rel 12, V1210. 2014;.

[56] Evolved Universal Terrestrial Radio Access (E-UTRA) and Universal Terrestrial Radio Access (UTRA); Radio Frequency (RF) requirement background for Active Antenna System (AAS) Base Station (BS) radiated requirements. 3GPP TR 37843, Tech Repo Rel 15, V1570. 2020;.

[57] Radio Frequency (RF) conformance testing background for radiated Base Station (BS) requirements. 3GPP TR 37941, Tech Repo Rel 16, V1661. 2020;.

[58] 5GS; User Equipment (UE) conformance specification; Part 1: Protocol. 3GPP TS 38523-1, Tech Spec Rel 16, V1650. 2020;.

[59] NR. User Equipment (UE) conformance specification; Radio resource management (RRM). 3GPP TS 38533, Tech Spec Rel 16, V1650. 2020;.

[60] NR. User Equipment (UE) radio transmission and reception; Part 1: Range 1 Standalone. 3GPP TS 38101-1, Tech Spec Rel 16, V1650. 2020;.

[61] NR. User Equipment (UE) radio transmission and reception; Part 2: Range 2 Standalone. 3GPP TS 38101-2, Tech Spec Rel 16, V1650. 2020;.

[62] NR. User Equipment (UE) radio transmission and reception; Part 3: Range 1 and Range 2 Interworking operation with other radios. 3GPP TS 38101-3, Tech Spec Rel 16, V1650. 2020;.

[63] NR. User Equipment (UE) conformance specification; Radio transmission and reception; Part 1: Range 1 Standalone. 3GPP TS 38521-1, Tech Spec Rel 16, V1650. 2020;.

[64] NR. User Equipment (UE) conformance specification; Radio transmission and reception; Part 2: Range 2 Standalone. 3GPP TS 38521-2, Tech Spec Rel 16, V1650. 2020;.

[65] NR. User Equipment (UE) conformance specification; Radio transmission and reception; Part 3: Range 1 and Range 2 Interworking operation with other radios. 3GPP TS 38521-3, Tech Spec Rel 16, V1650. 2020;.

[66] Study on test methods for New Radio. 3GPP TR 38810, Tech Repo Rel 16, V1661. 2020;.

[67] Study on enhanced test methods for FR2 NR Use. 3GPP TR 38884: Tech Repo Rel 17, V010. 2020;.